

ReputationPro: The Efficient Approaches to CTT Computation in E-Commerce Environments

Haibin Zhang^{*}
Macquarie University
Department of Computing
Sydney, Australia
haibin.zhang@mq.edu.au

Yan Wang
Macquarie University
Department of Computing
Sydney, Australia
yan.wang@mq.edu.au

Xiuzhen Zhang
RMIT University
School of Computer Science
and IT
xiuzhen.zhang@rmit.edu.au

Ee-Peng Lim
Singapore Management
University
School of Information System
eplim@smu.edu.sg

ABSTRACT

In e-commerce environments, the trustworthiness of a seller is utterly important to potential buyers, especially when the seller is unknown to them. Most existing trust evaluation models compute a single value to reflect the general trust level of a seller without taking any transaction context information into account. With such a result as the indication of reputation, a buyer may be easily deceived by a malicious seller in a transaction where the notorious *value imbalance* problem is involved, namely, a malicious seller accumulates a high level reputation by selling cheap products then deceives buyers by inducing them to purchase more expensive products.

In this paper, we first present a trust vector consisting of three values for Contextual Transaction Trust (CTT). In the computation of three CTT values, the identified three important *context dimensions*, including product category, transaction amount and transaction time, are taken into account. Meanwhile, the computation of each CTT value is based on both past transactions and the forthcoming transaction. In particular, with different parameters regarding context dimensions that are specified by a buyer, different sets of CTT values can be calculated. As a result, all these values can outline the reputation profile of a seller that indicates the dynamic trust levels of a seller in different product categories, price ranges, time periods, and any necessary combination of them. We term this new model as *ReputationPro*. However, in *ReputationPro*, the computation of reputation profile requires novel algorithms for the pre-computation of aggregates over large-scale ratings and

transaction data of three context dimensions as well as new data structures for appropriately indexing aggregation results to promptly answer buyers' CTT requests. Moreover, storing pre-computed aggregation results needs to consume a large volume of space particularly for a system with millions sellers. Therefore, reducing storage space for aggregation results is also a challenging demand.

To solve these challenging problems, we then propose a new index scheme *CMK-tree* by extending the *K-D-B-tree* that indexes spatial data to support efficient computation of CTT values. After that, we further extend *CMK-tree* and propose a *CMK-tree^{RS}* approach to reducing the storage space allocated to each seller. The two approaches not only are applicable to three context dimensions that are either linear or hierarchical, but also take into account the characteristics of the transaction-time model, namely, transaction data is inserted in nondecreasing time order. Moreover, the proposed data structures can index each specific product traded in a time period in order to compute the trust level of a seller in selling a product. Finally, the experimental results illustrate that the *CMK-tree* is superior in efficiency for computing CTT values to all three existing approaches in the literature. In addition, though with reduced storage space, the *CMK-tree^{RS}* approach can further improve the performance in answering buyers' CTT queries. Therefore, our proposed *ReputationPro* model is scalable to large-scale e-commerce websites in terms of efficiency and storage space consumption.

1. INTRODUCTION

In e-commerce environments, when a buyer needs to select a seller from a large pool of sellers, the trustworthiness of a seller is a crucial issue in decision-making [14, 19]. At eBay¹ with 233 million sellers and buyers, after each transaction, a buyer can provide a rating (+1, 0, or -1) to the centralized trust management system according to transaction quality. After accumulating over a time period, a single positive feedback rate is calculated to indicate the trust level of the seller in the latest time period (e.g. “the latest one month”, “six

^{*}Mr. Zhang is the corresponding author of this paper

¹<http://www.ebay.com/>

months” and “twelve months”). However, this simple trust management system is vulnerable to some frauds from malicious sellers [18, 31]. For example, a malicious seller can gain a good reputation by honestly selling good and low value (price) products. Once having accumulated a good reputation, s/he may deceive buyers by inducing them to buy more expensive products, but either not delivering the ordered product or else delivering a fake product. In the literature, this is referred to as the *value imbalance problem* [8, 18], and several real world cases have been reported [31]. For instance, an Australian deceiver at eBay tricked people for more than AU\$10K in total. A Californian deceiver cheated victims in transactions for exceeding US\$300K in total.

In view of the aforementioned problem, Zhang et al. [58, 60] have analyzed and summarized the following reasons in most existing trust evaluation models why they cannot identify *value imbalance* in transactions.

- *The lack of consideration of context in transaction trust evaluation:* In e-commerce environments, different transactions generally have different *natures* and *contexts*; even the same seller needs to be considered differently with regard to the trustworthiness in different forthcoming transactions [44, 43, 20, 30]. In fact, the *value imbalance problem* is only a type of the *context imbalance problem* [60] in transactions, where imbalance can also exist in product categories. For example, following a few cases of fraud at Alibaba², which supports both B2B and B2C online trading with 50 million users, buyers are explicitly reminded to manually check if the products being offered by a supplier fall into in the same categories as the products that the supplier usually sells³. This example also indicates that reputation-based transaction trust evaluation should be “transaction context-aware”.
- *The static trust evaluation result:* Most models compute a single trust value based on past transactions [33, 16, 47, 45, 41]. However, such a single value basically only reflects a seller’s general trust status, and is static with regard to any forthcoming transaction [43]. As illustrated above, different transactions may have different contexts. The static trust evaluation of a seller can hardly predict the likelihood of a successful forthcoming transaction. Thus, trust evaluation should be associated with both past transactions and the forthcoming transaction.

1.1 Motivation

Now, let us consider a simple example. Suppose a malicious seller S_1 has completed 198 transactions with good transaction quality selling “AT&T SIM Card” at the price of \$1 and obtained 198 positive ratings. The seller S_1 also has completed other 2 transactions with poor transaction quality selling “Apple iPhone5 16GB” at the price of around \$700 and obtained 2 negative ratings. Based on the trust evaluation model used at eBay, the trust level of S_2 is as high as 0.99. Next, consider a scenario that a buyer B plans to buy an “Apple iPhone5 16GB”. Meanwhile, the seller S_1 is selling this product, and the price \$700 offered by him/her

²<http://www.alibaba.com/>

³http://resources.alibaba.com/article/232530/Protect-yourself_from-fraudsters-pretending-to-be-Gold-Suppliers.htm

is cheaper than other buyers. Clearly, the seller S_1 is very attractive and appears to be trustworthy as well. Thus, the buyer B tends to buy the “Apple iPhone5 16GB” from S_1 . In such a case, the monetary loss of B is very likely to happen. However, in addition to the general trust value 0.99 to buyers, if B knew that S_1 received negative ratings in occurred transactions selling “Apple iPhone5 16GB”, B would not purchase from S_1 . In fact, from buyers’ point of view, they are more concerned about the trust level of a seller in a potential forthcoming transaction, rather than a general trust value resulting from all occurred transactions.

Suppose a seller S_2 has completed many more transactions in a long time period selling products in a variety of categories. When the buyer B plans to buy a “Canon EOS 6D SLR Digital Camera” at the price of around \$1600 from S_2 , in addition to the trustworthiness of S_2 in selling this product, B could also be concerned about the trustworthiness of S_2 in selling “Canon DSLR camera” with a price range of “\$1000-\$2000” (i.e. a query w.r.t. a higher layer in the hierarchical product category in a price range) in the latest 3 months or the latest 6 months. This is particularly the case when the product in the forthcoming transaction is just available in market and the number of existing transactions selling this product is quite low or even zero. If S_2 is reputable in all these related transactions, there should be good reasons for B to trust S_2 in a new transaction for purchasing a “Canon EOS 6D SLR Digital Camera” at the price of around \$1600. Otherwise, if S_2 has problems in the transactions in a certain product category or a certain price range (e.g., S_2 received a lot of negative ratings in the transactions in selling “Canon EOS 6D SLR Digital Camera”), it is necessary for trust evaluation to indicate the flaw of S_2 in reputation.

The above processing follows the suggestion from Alibaba website that a buyer needs to check if the product to be purchased from a seller is in the categories the seller usually sells and if the existing transactions in these categories are reputable. Similarly, as a buyer is very concerned about the possibility of monetary loss, trust evaluation needs to indicate trust levels over different price ranges, each of which takes the price of the product to be purchased as approximately the medium value. In addition to them, a further step is to evaluate trust over the combination of product category and price range as well as time period as different buyers buy products in different categories and with difference prices from the same seller. Such evaluation results can reveal potential risk if a seller has problems in reputation in the transactions in a product category, a price range and a time period, related to the potential new transaction that the buyer plans to complete with the seller.

Obviously, the afore-mentioned needs cannot be satisfied by any single-value trust valuation model. In the meantime, the new needs bring challenges in trust computation as a long-existing seller usually has large-scale transactions with a wide variety of product categories as well as a wide price range. Therefore, the computation of a seller’s trust levels in various transaction contexts incurs high complexity.

1.2 A Trust Vector based Framework and The Challenges in Computation

Based on the above examples and analysis, in contrast to most existing trust management models that compute a single trust value, our proposed framework is to compute a

trust vector for a seller [60]. The computation of trust values in the trust vector takes transaction context into account and is associated with a forthcoming transaction.

The trust vector consists of three major elements, which are called Contextual Transaction Trust (CTT) values. They are

1. *the trust level of a seller in selling a specific product to be traded in a forthcoming transaction;*
2. *the trust level of the seller in a layer in the product category hierarchy that is higher than the specific product to be traded in the forthcoming transaction, within a price range and a time period;*
3. *the trust level of the seller in a valid price range and a time period.*

When computing the last two elements, the parameters, such as product category, price range and time range, can be specified and adjusted by the buyer. For example, if “*Canon EOS 6D SLR Digital Camera*” is the product in the forthcoming transaction, the buyer can specify and adjust “*product category*” along a path in the product category hierarchy, such as, “*Canon DSLR camera*”, “*DSLR camera*” and “*Digital camera*”, in sequence. If the product is “*Apple iPhone5 16GB*”, the corresponding product categories will be “*Apple iPhone*” and “*Smartphone*” in sequence. Meanwhile, the buyer may also specify and adjust the price range and the time range. Each price range takes the price of product as approximately the medium value.

We use *granularity* to represent the differences in transaction context determined by a layer in the product category hierarchy, a price range and a time period. In addition, we term the query on CTT values as a *CTT query*, and term the computation of CTT values as *CTT computation*. Hence, with all computed trust results, the *reputation profile* of a seller can be outlined, which can indicate the dynamical trust levels of a seller in different products and product categories, price ranges, time periods and necessary combination of them, greatly help identify the value imbalance problem potentially existing in forthcoming transactions, and avoid monetary losses of buyers.

However, at e-commerce websites, a popular seller usually sells a wide variety of products distributed in different product categories. In addition, a large number of buyers can be accessing one seller’s reputation data with regard to their potential transactions. In order to promptly answer a buyer’s CTT requests, it is necessary to pre-compute aggregates over large-scale transaction data and ratings with necessary combinations of three context dimensions, i.e. product category, price and transaction time. Moreover, storing these aggregation results will consume a large volume of space particularly for a system with millions sellers. Thus, the *CTT computation* for outlining sellers’ reputation profiles is a very challenging problem that requires new data structures and novel algorithms that are scalable to large-scale e-commerce websites in terms of efficiency and storage consumption for CTT computation.

1.3 Our Approaches and Contributions

To solve the challenging CTT computation problem, we propose our model *ReputationPro* in this paper. Our work and contributions in *ReputationPro* are briefly summarized below:

(1) In contrast to most existing trust valuation models [33; 6; 16; 50; 48; 25; 41], our model considers three important context dimensions in e-commerce environments, i.e., *Product Category*, *Price* and *Transaction Time* (see Section 3), and it outlines the reputation profile of a seller which can indicate the dynamic trustworthiness in different product categories, price ranges, time periods, and any necessary combination of them (see Section 4).

(2) In the literature, our targeted CTT computation problem is similar to data warehousing and OLAP (On-Line Analytical Processing) technology [5] (see Section 2.2). In particular, the traditional RA (Range Aggregate) [27] in spatial data warehouses is relatively close to CTT computation. Typically, an RA query is in regards to the computation of the total number of points falling into a query region. Thus, we first present a review on popular approaches to the RA problem in two dimensional space and identify the limitations of these approaches in solving our targeted problem (see Section 2.3). Then, we further extend the RA problem in a two-dimensional space to CTT computation with the x-axis representing the *Transaction Time* dimension in days, the y-axis representing the *Transaction Amount* dimension, and the *Product Category* dimension taken as the extended third dimension (see Section 5).

(3) We point out that the characteristics of CTT computation are different from those of the traditional RA problem. Towards efficient CTT computation, we propose a new disk-based index scheme *CMK-tree* and a new query algorithm (see Section 6). The design of *CMK-tree* takes into account the special characteristics of CTT computation as follows:

- Different from the traditional RA problem that basically covers a two-dimensional space [27; 37], three transaction dimensions exist in CTT computation, i.e. Product Category, Price and Transaction Time. Although, with reduction techniques [54; 37], some existing approaches can be applied in three or higher dimensions, each dimension is linear in the traditional RA problem. By contrast, the Product Category dimension in CTT computation has a hierarchical structure.
- The CTT computation has the same characteristic as the transaction-time model [56], i.e. the records of newly happened transactions are inserted in chronological order.
- In the traditional two-dimensional RA problem [37], one point represents one object only (e.g., a car). By contrast, as a common case in e-commerce environments, a seller may have multiple transactions with the same price on a given day selling the same product, i.e. one point may represent multiple such transactions. The existing approaches to the RA problem focus on either indexing all the objects or overlooking the inserted objects themselves. Unlike these approaches, in CTT computation, we need a new index scheme that does not need to index all transactions but aggregates the repeated transactions on a given day, which sell the same product. In addition, the new index scheme should also guarantee that each specific product can be indexed in order to compute the trustworthiness of the seller in selling a product (see Section 4.3).

(4) Though three disk-based approaches have been proposed [61] to CTT computation taking into account the

above special characteristics, they have low efficiency of computing CTT values in some cases (see Section 2.5). By contrast, the new index scheme *CMK-tree* proposed in this article reduces computation time by 12.2%-66.7% on four large datasets. In particular, while answering a buyer's CTT queries for each brand-based product category, it has almost linear query performance (see Section 6.4). This is a significant advantage in answering CTT queries when a large number of buyers are accessing a seller's reputation data simultaneously.

(5) The existing approaches for CTT computation adopt a single fine time granularity and aggregate the ratings by days [61]. However, with continuous growth in transaction time (e.g., one year or two years) and significant increase of historical transaction data and ratings, the aggregation index with a single fine time granularity does not scale in terms of storage space. Here the *aggregation index* refers to the index containing some aggregates of ratings. To solve this problem, we further propose an approach *CMK-tree^{RS}* to reduce the storage space allocated to each seller for storing the aggregation index (see Section 7). The *CMK-tree^{RS}* takes into account the requirements of buyers' CTT queries, which maintains the aggregation index at different time granularities: recent ratings (e.g., "*the latest 3 months, i.e., the latest 90 days*") are aggregated at the fine time granularity of days, and earlier ratings (e.g., "*3 months ago, i.e., 90 days ago*") are aggregated at a coarse time granularity of weeks.

(6) We have conducted experiments on four large datasets with transactions of 12 months. The experimental results illustrate that the performance of *CMK-tree* is much better in efficiency than all three existing methods [61] in computing CTT values. In addition, our proposed *CMK-tree^{RS}* can significantly reduce the storage space allocated to each seller as well as the time of computing CTT values (see Section 8).

The rest of the paper is organized as follows. Section 2 provides a brief overview of related work. We introduce the modeling of transaction context in Section 3. In Section 4, we introduce our proposed trust vector and the *Reputation-Pro* model. Section 5 presents how to extend Range Aggregate (RA) in a two-dimensional space to CTT Computation. Section 6 proposes a new disk-based index scheme the *CMK-tree* in detail. Section 7 proposes an approach *CMK-tree^{RS}* to save storage space of aggregation index. While Section 8 evaluates our approach empirically, Section 9 concludes our paper.

2. RELATED WORK

This section reviews related work in three aspects. First, Section 2.1 reviews some existing trust evaluation models. Second, Section 2.2, Section 2.3 and Section 2.4 review the related techniques in data warehousing. In these sections, we also focus on identifying the limitations of these techniques in resolving our targeted CTT computation problem. Finally, Section 2.5 reviews the existing approaches to CTT computation.

2.1 Trust Evaluation

2.1.1 Trust Evaluation without Contextual Information

In most trust evaluation models [52; 6; 49; 16; 47; 40; 48; 38; 45; 21; 12], a single trust value (e.g., a value in the range $[0, 1]$) is computed to reflect the "general" or "global"

trust status of a target accumulated in a certain time period. They have been proposed in various application fields. Specifically, in Peer-to-Peer (P2P) network, [16] propose the EigenTrust model, and a "global" trust value of a given peer is calculated via collecting binary trust ratings. [50] propose a PeerTrust model which defines some general trust metrics and formulae to aggregate ratings into a final trust value. [12] also use a single general value to evaluate the trustworthiness of each peer in P2P network. In the field of service-oriented computing (SOC), [45] propose some trust evaluation metrics and a formula for trust computation, with which a final trust value is computed. [38] introduce the Trust and Reputation model for Agent-based Virtual OrganisationS (TRAVOS) system which calculates an agent's general trust using probability theory, taking into account the past interactions between agents.

In addition, the subjective property of trust is introduced for rating aggregation, e.g., the work in [13; 46], where the subjective probability theory is adopted in trust evaluation. [7] take advantage of fuzzy models and use membership functions to determine the trustworthiness of targets. [41] propose a trust evaluation model RLM which can be utilized to resist malicious feedback ratings. To sum up, these models do not take any contextual information into account. As a result, if applied in e-commerce environments, they can hardly predict the likelihood of a successful forthcoming transaction.

2.1.2 Trust Evaluation with Contextual Information

In the literature, [10] proposes a Multi-Dimensional Trust (MDT) model, which studies contextual trust from a multiple-faceted perspective. The trustworthiness of a particular task can be modeled in several dimensions (e.g., timeliness, quality and cost), letting a user specify the weight of each dimension for trust evaluation based on the personal preference. Thus, given the same seller, the trust results computed for different buyers may vary. Similarly, in REGRET [33] and RATEweb systems [25], a multi-dimensional structure is adopted when evaluating a seller's reputation. However, these models still focus on how to compute a single general or global trust value, and overlook that the transaction context (e.g., product category and transaction amount) may change in historical transactions. Therefore, they still can hardly predict the likelihood of a successful forthcoming transaction.

In recent years, more studies pay attention to introducing transaction context in trust evaluation in e-commerce environments [50; 23; 44; 20; 58; 24]; nevertheless, in-depth discussions and solutions are needed to focus on how to differentiate transaction contexts and take into account their impacts on trust evaluation. [30] propose a context-sensitive trust evaluation model (IHRTM) taking advantage of statistical relational learning. In the IHRTM model, contextual information is discussed in the *Seller* \times *Item* space. According to the learning results, all 47 selected sellers in their experiments are assigned to 4 groups based on the context attributes in the *Seller* space, such as feedback score and positive feedback rate, and the 630 items sold by these sellers are assigned to 40 clusters based on the context attributes in the *Item* space, such as product category and product condition (new or used). Finally, a 4×40 matrix is formed to indicate the trustworthiness of 4 seller clusters under 40 item clusters. However, IHRTM model has the following

drawbacks. First, in IHRTM, all sellers in one group have the same level of reputation in all 40 clusters of products, namely, given any one out of 40 item clusters, all sellers in a group either do not sell anything in the product cluster, or all have the same reputation over the items in the same cluster. When having a large number of sellers, there will be many clusters of sellers, leading to a high complexity in learning iterations. As new transactions happen every-day, the cost of re-learning which takes new transactions into account is high. Second, it does not support the analysis of reputation on the product categories along a path in the product category hierarchy (e.g. “Apple iPhone” and “Smartphone” in sequence). This analysis is especially necessary when a new product or a product in a new category is just released. Third, it does not support the trust evaluation of a seller in the transactions in a given price range. This need comes from a buyer when s/he is very concerned about the risk of monetary loss in a forthcoming transaction [50; 35]. By contrast, our *ReputationPro* model can outline a seller’s reputation profile and indicate his/her dynamic trustworthiness in different product categories, price ranges, and time periods.

In addition, the context similarity calculation is regarded as an important means to deal with the contextual trust evaluation problem. [39] propose a CAT (Context-Aware Trust) model to compare the similarity of contexts by using key values that can describe a specific context at least partially. [29] propose a trust model to resolve contextual trust, using clustering to identify the full context space as several reference contexts based on the context attributes. The trust evaluation of a new context is the weighted sum of the trust values in all reference contexts. As pointed out by [26], the context similarity is used to infer the trustworthiness of a target in a certain context where there are no or not enough ratings from the same context. Therefore, these trust models still focus on calculating a single trust value under corresponding specific context. However, they are different from our *ReputationPro* model proposed in this article, which aims to promptly answer a buyer’s CTT queries on a seller’s trustworthiness in various transaction contexts. Instead of providing only a single value, our approach computes sets of trust values to outline the reputation profile of a seller. Clearly, it is more comprehensive for our approach to indicate the trustworthiness of a seller for a forthcoming transaction.

2.2 OLAP (On-Line Analytical Processing) and Data warehouses

In a wider research literature, our targeted problem of CTT computation is somewhat similar to sales analysis from multiple perspectives in data warehouses and business intelligence. Typically, the sales data warehouse for a company contains three dimensions *Product category*, *Location* and *Time*. The OLAP operations refer to the queries on the aggregation of sales over each dimension or their combinations, such as the sum of sales per product category or the sum of sales per product category and per month combination. Gray et al. [9] point out that there are $O(2^n)$ possible aggregations for a data warehouse with n dimensions composing a “data cube”.

In order to accelerate query processing, some results can be pre-computed and stored as *materialized views* [11; 22]. However, these approaches only benefit the queries on di-

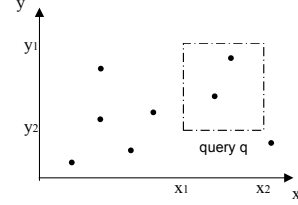


Figure 1: An example of an RA query

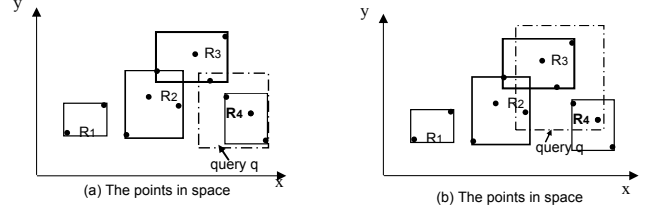


Figure 2: An aR-tree

mensions with predefined hierarchies. In particular, the Time dimension in sales analysis refers to static calendar months, e.g., January, February, etc. By contrast, in CTT computation, while the product category hierarchy is predefined and static, Price and Transaction Time are dynamic dimensions (see Section 3). Specifically, the dynamicity of the Price dimension refers to the price of a product may change over time. Even on a given day, multiple transactions selling the same product may have different prices. In addition, the dynamicity of the Transaction Time dimension refers to the new transactions added to the database over time modifying the set of “most recent transactions”.

Moreover, some existing work improves the performance of queries in data based on specifically designed column-oriented database systems [1]. Different from their work, our approach in this article is based on popular relational database management systems that are being widely used by e-commerce websites, so that the designed models can be directly applicable.

2.3 The RA Query

In the literature, the RA (Range Aggregate) problem in spatial data warehouses is relatively close to our targeted CTT computation problem (see Section 5), as it aggregates data in dynamic dimensions. Because of this characteristic, we review the approaches to RA problem separately.

Fig. 1 shows the traditional RA query [27] in a two-dimensional space which is in regards to computing the total number of points falling into a query region q surrounded by $[x_1, x_2]$ and $[y_1, y_2]$, e.g., answering a query in traffic supervision systems, such as: “What is the total number of cars inside a certain district?”. Usually, a query region can be any area within the two-dimensional space. To accelerate query processing, most existing works still pre-compute some results, but they appropriately store the results in the specialized index [28, 37, 36, 56]. Considering the memory-based approaches are inappropriate for large-scale data processing, in this subsection, we briefly review some well-known disk-based approaches.

2.3.1 The aR-tree

The *aR-tree* [15, 27] maintains the x-y coordinates for each minimum bounding rectangle (MBR) (e.g., R_1 , R_2 , R_3 , R_4

Figure 3: An RA query transformed to two Vertical Range Aggregate (VRA) queries

in Fig. 2(a) are all MBRs). Meanwhile, each MBR records the total number as an aggregate of the objects that fall into an MBR. To compute the number of objects in a query region q , in Fig. 2(a), the MBR R_4 within q will not be accessed. Rather, R_4 's pre-computed aggregate (i.e. 3) is directly used. But R_3 needs to be visited, as it partially overlaps with q . The total number of points in q equals their sum $3 + 1 = 4$. A serious problem of the *aR-tree* is that its performance significantly degrades when answering a large query region, since in such a case there are more MBRs overlap with the query region (see Fig. 2(b)).

2.3.2 The *aP-tree*

Tao et al. [37] propose the *aP-tree* to improve the *aR-tree*, based on the following transformation on a query region q . They first convert each spatial point to an *interval* (i.e. a horizontal line) (see Fig. 3(b)). When q surrounded by $[x_1, x_2]$ and $[y_1, y_2]$ is transformed to two *borders* (i.e. two vertical lines): $x_1 : [y_1, y_2]$ and $x_2 : [y_1, y_2]$, an RA query is converted to retrieving the number of intervals that intersects the two borders. For instance, in Fig. 3, the number of intervals intersecting the left border $x_1 : [y_1, y_2]$ is 3 while the number of intervals intersecting the right border $x_2 : [y_1, y_2]$ is 5. The total number of points in q equals their difference $5 - 3 = 2$. Tao et al. [37] define the number of intervals intersecting a border as a Vertical Range Aggregate (VRA). In order to compute each VRA value, the *aP-tree* is then proposed that contains an additional field *agg* in each entry, extending the *multiversion B-tree* (MVBT) [4].

In order to answer an RA query, the *aP-tree* indexes all the objects [56, 61]. As shown in Fig. 1, in the traditional RA problem, one point in a two-dimensional space represents one object only (e.g., a car). However, in our targeted CTT computation problem, one point may represent multiple such objects. For example, it is quite common that a seller has multiple transactions with the same price selling the same product on a given day. Here the x-axis represents days, and the transactions occurred on the same day have the same x-coordinate. In this case, a new index scheme should be proposed to take this characteristic into account. Unlike the *aP-tree*, the new index does not need to index all the transactions; rather, multiple repeated transactions should be aggregated, and then the new index only needs to store the aggregation results.

2.3.3 The *MVSB-tree* and The *BA-tree*

Zhang et al. [56] address the RA problem in a two-dimensional space by converting an RA query to four dominance-sum queries. Given two two-dimensional points $x = (x_1, x_2)$ and $y = (y_1, y_2)$, x dominates y if $x_1 \geq y_1$ and $x_2 \geq y_2$. The

corresponding dominance-sum of the point P is the aggregation of all the points that are dominated by P . Therefore, in Fig. 4(a), the total number of points in the query region $P_1 P_2 P_3 P_4$ equals $7 - 5 - 2 + 2 = 2$, namely, the dominance-sum of the point P_2 (see Fig. 4(b)) subtracts the dominance-sum of the point P_1 (see Fig. 4(c)) and the dominance-sum of the point P_4 (see Fig. 4(d)). As the dominance-sum of the point P_3 (see Fig. 4(e)) has been subtracted twice, their sum must be added again. In order to compute each dominance-sum query, Zhang et al. further propose the *MVSB-tree* [54, 56] and the *BA-tree* [55], respectively.

The *MVSB-tree* results from augmenting the *SB-tree* [51]. It logically divides the two-dimensional space into multiple nonintersecting rectangles. When inserting an object with the coordinate (x_i, y_i) , the aggregation operations perform in all the rectangles within the area $[x_i, max_x] \times [y_i, max_y]$. Here the max_x and max_y collectively form the upper-right corner of the complete space. Although the *MVSB-tree* considers a point may represent multiple such objects, it overlooks the inserted objects themselves. If it is applied to CTT computation problem, each specific product cannot be indexed. As a result, computing the trust level of a seller in selling a product cannot be fulfilled. Furthermore, the *MVSB-tree* is particularly designed for solving the dominance-sum problem. Thus, four dominance-sum queries are needed to answer an RA query (see Fig. 4). By contrast, our proposed new index scheme answers only two VRA queries for the same purpose (see Fig. 3).

The *BA-tree* is another index scheme for answering RA queries that extends the *K-D-B-tree* [32]. Fig.5 depicts a general structure of *BA-tree*, as in the *K-D-B-tree*, each node corresponds to a rectangular space, such as the area A . The node at a higher level corresponds to a larger rectangular space formed by several adjacent areas, such as the area formed by A , B and C . The root node corresponds to the complete space. The augmentation of the *BA-tree* over the *K-D-B-tree* is that each node (e.g., the area D) also stores three aspects of information: the subtotal of points to the lower left of D (see Fig. 5(a)), the x-coordinates of the points below D (see Fig. 5(b)) and the y-coordinates of the points to the left of D (see Fig. 5(c)). The *BA-tree* achieves linear performance when answering each dominance-sum query. However, as pointed out by [56], it does not fit for the transaction-time model where the records of newly happened transactions need to be inserted in the nondecreasing time order.

2.4 Hierarchical Temporal Aggregation with Fixed Storage Space (HTA^{FS})

The more general problems in range aggregate (RA) are the range-temporal (two dimensions with one as the time dimension) and spatio-temporal (three dimensions with one as the time dimension) aggregations. In the literature, some index schemes have been proposed to solve these aggregation problems [54, 55, 36]. However, all these approaches do not have restriction on storage space to store aggregation index. As a result, with continuous growth in time dimension (e.g., one year or two years) and significant increase of historical data, the aggregation index can easily become large in the size of consumed space.

In contrast to the above existing approaches, Zhang et al. [53] propose a Hierarchical Temporal Aggregation model with fixed storage space (denote as HTA^{FS}) to control stor-

Figure 5: The structure of $BA\text{-tree}$

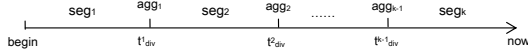


Figure 6: A general structure of HTA^{FS} model

age space of aggregation index over data streams. Fig. 6 depicts the general structure of the HTA^{FS} model to deal with points aggregation in a one-dimensional space. A k -level time hierarchy, where $gran_1$ is at the coarsest time granularity (e.g., by days) and $gran_k$ is at the finest granularity (e.g., by seconds). Suppose that the HTA^{FS} model divides the time space $[begin, now)$ into k segments. Each segment seg_i ($i = 1, 2, \dots, k$) maintains the corresponding aggregations with the time granularity $gran_i$. The term *begin* denotes the starting time and *now* denotes the increasing current time. New objects are inserted with the point “now” moving to the right in the x-axis. The constraint for the HTA^{FS} model is that the size of available storage space is fixed. When the size of total storage becomes more than a threshold S , older information is aggregated at a coarser granularity of time.

In [57], we have applied the HTA^{FS} model to CTT computation and proposed a model named CTT^{FS} . Similarly, in the CTT^{FS} model, transaction data and ratings are also aggregated at different time hierarchies. Moreover, compared with original HTA^{FS} model, the additional characteristics in CTT computation are identified. As a seller has imbalanced transaction volume within each product category, a dynamic storage space allocation strategy is first proposed. More specifically, for the product category on which a seller has numerous transactions, more space should be allocated for storing the aggregation index. If the size of the aggregation index for this product category becomes larger than the allocated storage space. Then, earlier ratings are aggregated at a coarser time granularity. To sum up, the CTT^{FS} model also guarantees a fixed storage space allocated to a seller for CTT computation. Although the CTT^{FS} model can save the storage space to some extent, we will analyze that the strategy of allocating the fixed storage space is unreasonable for our targeted CTT computation problem in

Section 7. Thus, unlike the CTT^{FS} model, a new solution $CMK\text{-tree}^{RS}$ is proposed to reduce storage space consumption in this article.

2.5 Existing Approaches to Contextual Transaction Trust Computation

In the literature, we have proposed a preliminary trust vector which takes transaction context factors into account in the computation of contextual transaction trust values (CTT values), and then we have introduced the first set of technical solutions to compute CTT values [59]. In [60], more details of our proposed trust vector based framework for CTT computation are presented. In particular, we have conducted empirical studies to compare the trust vector with some typical single-value trust valuation models [33, 48] to illustrate its advantages. After that, we have further extended our work [59] by introducing a new product category hierarchy for supporting finer-grained analysis on the transaction trust of a seller as well as aggregating repeated transactions and have proposed three new disk-based index schemes *eaR-tree*, *eaP-tree* and *eH-tree* for CTT computation [61]. All these approaches can meet the requirements for answering a buyer’s CTT queries on the dynamic trust levels of a seller in different product categories, price ranges and time periods. However, they have poor performance in some cases. Specifically, as the *eaR-tree* extends the *aR-tree*, the query cost for *eaR-tree* depends on the size of the CTT query region formed by the price range and transaction time range: the larger the query region, the worse the performance in answering a CTT query. For both the *eaP-tree* and the *eH-tree* that extend the *aP-tree*, they index all the transactions and cannot essentially aggregate repeated transactions that occurred on a day, leading to the inferior performance.

In the new disk-based index scheme *CMK-tree*, the above problems will be solved. Like the *BA-tree* [55], the *CMK-tree* extends the *K-D-B-tree*, however, it adopts a different extension strategy that is particularly designed to efficiently support the computation in answering a buyer’s CTT queries. Moreover, all the existing approaches aggregate the transaction data and ratings at the granularity of a day. As mentioned in Section 2.4, they lead to the problem of large space consumption when dealing with a large number of sellers. Therefore, we further propose the $CMK\text{-tree}^{RS}$ to reduce storage space allocated to each seller for storing the aggregation index.

3. TRANSACTION CONTEXT

In our previous work [60], we have identified three important *context dimensions* with influence on the trustworthiness of a forthcoming transaction. They are *product category*, *transaction amount* and *transaction time*. The context

Figure 7: Part of product category hierarchy for the segment “Information, communication and media”

of a transaction can be represented as different layers in the product category hierarchy and different ranges in each of the Price dimension and Transaction Time dimension.

- **Product Category (a static but hierarchical dimension):** The category of transaction items has a hierarchical structure. There are some *Products and Services Categorization Standards (PSCS)* that aim at constructing the product category hierarchy, such as UNSPSC⁴ and eCl@ss⁵, each of which groups similar products and provide an industry-neutral hierarchical structure of product categories with up to four layers. eBay has a different schema with simply two layers in product category⁶, and it groups products by considering some factors such as marketing and common use.

We establish the product category hierarchy for the analysis of dynamic reputation of a seller. We extend eCl@ss due to its reasonable classification in practice, i.e. products in eCl@ss are more functionally grouped, and they are subdivided for specific usage. For example, in eCl@ss, “Digital Camera” can be further classified as “DSLR (Digital single-lens reflex cameras)”, “Compact Digital Camera” and “Mirrorless Digital Camera”. But it is not subdivided in both UNSPSC and eBay. In addition, we sort out the logical relations between product categories in eCl@ss. Then, we add the attribute “Brand” to the product category hierarchy to support finer-grained analyses on transaction trust with “drill down” and “roll up” operations in the hierarchy. Under each brand, there are corresponding products that belong to this brand.

Fig. 7 presents a small part of our extended product category hierarchy. For instance, if the product is “Apple iPod nano 16GB (mc696ll/a)”, then its ancestors in the product category hierarchy are “Apple MP3 player (iPod)” and “MP3 player” in sequence. If the product is “Apple iPhone5 16GB”, then its ancestors in the product category hierarchy are “Apple iPhone” and “Smartphone” in sequence. The category hierarchy for the product “Canon EOS 6D SLR

Digital Camera” is complex that has several layers, and its ancestors are “Canon DSLR camera”, “DSLR camera” and “Digital camera” in sequence. In our extended hierarchy, each product category has a unique id termed as *C-value* (see Fig. 7), with which a layer, the layer’s parent and children can be located.

- **Transaction Amount and Transaction Time (two dynamic linear dimensions):** Transaction amount refers to the sum of the prices of all products in a transaction. A transaction of about \$10 is obviously different from one involving \$10K. The larger the transaction amount, the more likely a fraudulent action may occur since the potential benefit of the fraud is greater [2]. For the sake of simplicity, like eBay, *each item in a transaction is considered separately* in our work. A transaction with multiple transaction items are taken as several transactions separately with one item each. Hence, the transaction amount equals the price of the product in a transaction. In this paper, we use “transaction amount” and “price” interchangeably. Transaction time is the time when a transaction happens. Trust evaluation is time-sensitive, because the transaction quality may change over time [34].

The Price dimension is dynamic as the price of a product may vary from time to time. Owing to product condition (new and used) and product value changes over time, the prices of transactions selling the same product may be different. Also, a buyer’s queries on a price range can vary with the same product, or vary from product to product. For instance, the price of a product that a buyer wants to buy from a seller is around \$500, and the buyer may be concerned about the trustworthiness of this seller on selling products at a price range of “\$400-\$600” or “\$350-\$650”. If the price of another product is \$1500, the corresponding price range in a query may be “\$1000-\$2000”, taking \$1500 as the medium value.

The Transaction Time dimension has a specific characteristic in trust computation. Any CTT queries on the transaction time range starts from a previous point and ends at the point “now”, i.e. a query regarding the reputation in the recent transactions, such as “the latest 1 month”, “the latest 3 months” and “the latest 12 months”. In addition, Transaction Time dimension is also dynamic because the time point “now” changes everyday, and new transactions added to the database over time change the set of “most recent transactions”.

4. A TRUST VECTOR BASED FRAMEWORK FOR OUTLINING REPUTATION PROFILE

In this section, we first define the data that are needed for CTT computation. We then present a trust vector which consists of three CTT values and introduce why they can be used to outline the reputation profile of a seller.

4.1 Trust Data Representation

The following data elements are needed for CTT computation.

$$TR^{(t)} = \langle S; B; p; C\text{-hierarchy}; ta; t; r \rangle \quad (1)$$

- $TR^{(t)}$ is a transaction between a seller S and a buyer B happening at time t ;

⁴<http://www.unspsc.org/>

⁵<http://www.ecl@ss.de/>

⁶<http://pages.ebay.com/sellerinformation/ebaycatalog/categories.html>

- p is the product (i.e. transaction item) traded in the transaction $TR^{(t)}$;
- $C-hrchy$ represents the path in product category hierarchy to which p belongs;
- ta is the transaction amount in transaction $TR^{(t)}$ for p ;
- r is a rating (an integer in a range, e.g., $\{-1, 0, 1\}$ or $\{1, 2, 3, 4, 5\}$) that the buyer B gives to the seller S for $TR^{(t)}$ to reflect a seller's performance during the whole transaction;
- A set of n past transactions can be denoted as $Trans = \{TR^{(t_1)}, TR^{(t_2)}, \dots, TR^{(t_n)}\}$.

4.2 CTT metrics

In the literature, existing studies average the rating values for calculating the trust value [33, 16, 49, 50, 47, 42, 25, 12]. Following this idea, in our model, we calculate each CTT value as the average of the ratings in a specific transaction context. Thus, two aggregates are pre-computed and stored separately. They are $count_r$, the number of ratings of the corresponding transactions, and sum_r , the sum of ratings in a specific layer of product category hierarchy within a specific transaction price range and a specific time period. With a pair of $count_r$ and sum_r , accordingly, the trust value can be computed as $T = \frac{sum_r}{count_r}$. In addition, based on the parameters of a CTT query, a set of $\{count_{r_i}, sum_{r_i}\}$ can be returned. Accordingly, the trust value is $T = \frac{\sum sum_{r_i}}{\sum count_{r_i}}$.

4.3 A Trust Vector

Our proposed trust vector [60] consists of three major CTT values.

(a) **Transaction Item Specific Trust (TIST)**: TIST is the average of all the ratings $\{r^{(t)}\}$ in the past transactions $Trans$ for trading the same transaction item p as in a forthcoming transaction.

(b) **Product Category based Trust (PCT)**: PCT is the average of all the ratings $\{r^{(t)}\}$ of the past transactions $Trans$ for selling the products in a product category (e.g., “Canon DSLR cameras” or “DSLR cameras”) above p (e.g., “Canon 6D DSLR camera”) in the product category hierarchy (see Fig. 7). When computing PCT, a price range covering the price a and a time range can be specified as the parameters. The variables p and a come from the context of the forthcoming transaction.

(c) **Similar Transaction Amount based Trust (STAT)**: STAT is the trust value of a seller in a specific price range covering price a and a time range. STAT is important for analyzing the trust level of a seller in different price ranges.

4.4 ReputationPro

In the above trust vector, all three CTT values are associated with both past transactions and the forthcoming transaction. With the same seller but a different forthcoming transaction, the computed trust values may be different. Even with the same forthcoming transaction, the trust values can vary. This is because a buyer can specify and change a layer in the product category hierarchy, a price range and a time period for computing the last two CTT values: PCT and STAT. With the combinations of the parameters specified in all three context dimensions, different sets of CTT

values can be computed, all of which can outline the reputation profile of the seller indicating the trust levels in various types of transactions. Thus, our *ReputationPro* model can greatly help detect the possibility of context imbalance problem in a forthcoming transaction.

5. EXTENDING TWO-DIMENSIONAL RANGE AGGREGATE FOR CTT COMPUTATION

In this section, we first discuss the relationship between two-dimensional RA problem and our targeted CTT computation problem. In Section 3, we have introduced that transaction context includes a static and hierarchical dimension, i.e. product category hierarchy, and two dynamic dimensions, i.e. transaction amount and transaction time. When computing PCT and STAT values, a CTT query covers both the Transaction Amount (Price) dimension and the Transaction Time dimension. Similar to the case depicted in Fig. 1 in Section 2.3, a CTT query can be first regarded as an RA problem in a two-dimensional space, where the x-axis represents the Transaction Time dimension in days and the y-axis represents the Transaction Amount dimension. Consequently, a CTT query on a seller in a time range $[t_1, t_2]$ and a transaction amount range $[ta_1, ta_2]$ can be converted by computing the number of the ratings $count_r$ and the sum of the ratings sum_r of the transactions that fall into the query range formed by $[t_1, t_2]$ and $[ta_1, ta_2]$.

Here, for further analysis, we need to point out that each point in a two-dimensional space represents one transaction or a set of transactions. There are three cases that should be differentiated.

Case 1: Given one point at (t_i, ta_i) , it may represent only one transaction that occurred on a day t_i with the transaction amount ta_i .

Case 2: As mentioned in Section 1.3, one point at (t_i, ta_i) may represent a set of repeated transactions that occurred on a day t_i selling the same product with the same price ta_i . In such a case, we need data structures to aggregate these repeated transactions.

Case 3: Given one point at (t_i, ta_i) , it may represent a set of transactions that occurred on a given day t_i selling different products with the same price ta_i . In such a case, they should be regarded as different transactions and aggregated separately.

Note that owing to product condition (new and used) and product value changes over time, the prices of transactions selling the same product may be different. In such a case, we regard them as different transactions and aggregate them separately.

Second, we introduce how to extend the two-dimensional RA problem to CTT computation after taking into account the product category hierarchy as the third dimension:

Step 1: Each transaction has a numeric string $C-hrchy$ to represent the path in the product category hierarchy to which the product traded in the transaction belongs;

Following the eCl@ss introduced in Section 3, a two-digit number is added to each layer of the product category hierarchy. Thus a unique $C-value$ is assigned to each product category. For example, in Fig. 7, the node “MP3 player” at layer 4 has the $C-value$ of “19081009” representing the

Figure 8: The structure of our proposed CMK-tree

$\langle C\text{-value}, [ta_{min}, ta_{max}], [t_{min}, t_{max}], count_r, sum_r, pointer \rangle,$

where the *C-value* denotes the unique id of the product category within the product category hierarchy; $[ta_{min}, ta_{max}]$ and $[t_{min}, t_{max}]$ are transaction amount range and transaction time range of all the transactions belonging to the current product category; *count_r* and *sum_r* denote the aggregates over these transactions; *pointer* points to its child, which is an R-node or an I-node. Therefore, an R-node contains multiple product categories represented by corresponding records, and these product categories are on the same layer within product category hierarchy. All R-nodes form an *N-ary tree*, and we term it as a *C-tree (product category tree)*.

6.1.2 The MK-tree

In addition to a *C-tree* consisting of R-nodes, following Step 3 in the extension process, each record in an R-node at brand-based product category layer (i.e. the bottom of the *C-tree*) points to a subtree that is external to the *C-tree*. Specifically, the design of each such subtree is based on extending the original *K-D-B-tree* [32] that is used for indexing spatial data.

The *K-D-B-tree* partitions a two-dimensional space into multiple nonintersecting rectangles (see Fig. 10(a)). Each record in a node in the *K-D-B-tree* corresponds to a rectangular space. Unlike the general structure depicted in Fig. 10(a), a special case “*domain 0*” *K-D-B-tree* has been proposed in [32]. In particular, for a general *K-D-B-tree*, a rectangular space can be split along any dimension (e.g., x-axis or y-axis). In contrast, for a “*domain 0*” *K-D-B-tree*, the space cannot be split along a specific dimension. For example, in Fig. 10(b), instead of dividing x-axis, the split can only be operated along the y-axis.

In the *CMK-tree*, the idea of “*domain 0*” *K-D-B-tree* [32] is adopted to generate each subtree to extend the *C-tree*. Since the x-axis (Transaction Time dimension) continuously moves to the right in our targeted problem, each subtree can be considered as a multi-version structure that makes *partial persistence*⁷ [56] a “*domain 0*” *K-D-B-tree*. In order to further demonstrate the structure of a subtree, we assume that each point in a two-dimensional space depicted in Fig. 11(a) represents a transaction, and all the transactions belong to the same brand-based product category. Correspondingly, in the subtree generated by these transactions (see Fig. 11(a)), a record in the node *X* surrounds the

⁷*partial persistence* implies that updates are only applied to the latest version of the data structure, creating a linear ordering of versions.

Figure 10: A special case of K-D-B-tree

rectangular $a_1a_2a_3a_4$ (R_1). This is the first version of “domain 0” *K-D-B-tree* as illustrated in Fig. 10(b). Another record in the node X surrounds the rectangular $b_1b_2b_3b_4$ (R_2) which is the second version. The record in the node Z at a higher level surrounds a larger rectangular space formed by $a_1a_2b_3b_4$. Furthermore, like the transformation given in Section 2.3.2, each transaction will generate an interval along the Transaction Time dimension (see Fig. 11(b)). As an extended structure, each record simultaneously maintains the transactions whose generated intervals intersect with the left border of the corresponding rectangle. For example, in Fig. 11(b), the record surrounding the rectangle $b_1b_2b_3b_4$ also stores the aggregates of transactions α_1 , α_2 and α_3 whose generated intervals along the Transaction Time dimension intersect with the left border b_1b_2 as well as the indexes of these three transactions for computing the trust level of the seller in selling a specific product. To facilitate discussion, we term such a subtree, i.e. an extended *Multi-version “domain 0” K-D-B-tree*, as *MK-tree*.

Next, we introduce the I-nodes and the L-nodes of an *MK-tree*. Based on the above description, the record in an I-node In_i (see Fig. 9(b)) has the form

$$\langle [ta_{min}, ta_{max}], [t_{min}, t_{max}], count_r, sum_r, P_i, Q_i \rangle ,$$

where $[ta_{min}, ta_{max}]$ and $[t_{min}, t_{max}]$ surround each nonintersecting rectangle; the term P_i is a pointer pointing to its child, which is an I-node or an L-node; the term Q_i is another pointer pointing to an aB^+ -tree that derives from the B^+ -tree [3]. As stated before, the purpose of building an aB^+ -tree is to index the transactions whose generated intervals along the Transaction Time dimension in-

tersect with the left border of the rectangle surrounded by $[ta_{min}, ta_{max}]$ and $[t_{min}, t_{max}]$. In the meantime, the aggregates over these transactions are maintained in $count_r$ and sum_r . Specifically, each aB^+ -tree is built in the separate transaction amount space. Like the B^+ -tree, the records in an aB^+ -tree are kept sorted based on their transaction amount (price). Also, each node in an aB^+ -tree has the same structure that consists of multiple records, each of which has the form $\langle price, count_r, sum_r, pointer \rangle$ (see Fig. 9(b)). The *pointer* points to its child, but for the records at leaf level, *pointer* points to the transaction record stored in the database. Note that each generated aB^+ -tree is based on the transactions in a brand-based product category. In addition, unlike the original B^+ -tree, the number of records to be inserted in an aB^+ -tree may be larger than the number of distinct values of transaction amount (y-coordinates) due to the reason of *Case 3* as illustrated in Section 5.

Moreover, when building an *MK-tree*, in order to avoid duplication of aB^+ -trees, the I-nodes actually include two types: (1) the I-node pointing to aB^+ -trees, and (2) the I-node without pointing to aB^+ -trees. To differentiate the above two situations, we call the I-node ‘L-I-node ($In(L)$)’ if its children are L-nodes, and ‘I-I-node ($In(I)$)’ otherwise. Therefore, the I-node depicted in Fig. 9(b) is an L-I-node $In(L)_i$. These two node structures will become clearer after introducing insertions in the next subsection.

Each record appearing in an L-node Ln_i (see Fig. 9(c)) also contains $count_r$ and sum_r because of aggregating the repeated transactions with the same price on a given day which sell the same product. It has the following form

$$\langle price, time, count_r, sum_r, pointer \rangle ,$$

where the *pointer* points to the transaction record stored in the database.

6.2 The Construction of a CMK-tree

This section formally describes the insertion operations for the *CMK-tree* which is to insert a transaction including the path in the product category hierarchy to which the product traded in the transaction belongs ($C-hrchy_i$), transaction amount (ta_i), transaction time (t_i) and the rating for the transaction (r_i). Meanwhile, the transaction records need to be inserted in the nondecreasing time order.

6.2.1 Insertion

Before inserting the data of a newly happened transaction into a *CMK-tree*, a path is first searched in a *C-tree*

Figure 12: The state of a CMK-tree after inserting three transactions

from top (the product category root) to bottom (the brand-based product category) (see Fig. 8) based on the *C-hrchy* of the transaction. If the product in the transaction belongs to a new product category on which the seller has no prior transactions, the new records are generated for this product category as well as its sub-categories and inserted to the corresponding R-nodes. Otherwise, the set of ranges and aggregates (i.e., $[ta_{min}, ta_{max}]$, $[t_{min}, t_{max}]$, $count_r$, sum_r) maintained in each record along the path are updated accordingly. After that, the insertion operations should be performed in an *MK-tree* pointed by the corresponding record in an R-node at the brand-based product category layer. Fig. 12 depicts the state of a *CMK-tree* after inserting the data of three transactions trading different products, which belong to the same product category with the same *C-hrchy*. In addition, the information $\langle ta_i$ (transaction amount), t_i (transaction time), r_i (rating) \rangle of three transactions is $\langle 5, 1, 1 \rangle$, $\langle 15, 1, 1 \rangle$ and $\langle 10, 2, 1 \rangle$.

6.2.2 Split

The split of an R-node is relatively simple. Unless stated otherwise, in the following example, we assume the capacity of all the nodes is five. In addition, the field sum_r in all the records is ignored, and we only use the field $count_r$ as the example to illustrate the aggregation process. Fig. 13(a) shows an example of the R-node split where Rn_1 is an R-node containing a record $\langle C-value_p, [10, 60], [1, 5], 32 \rangle$ at a higher level of the *C-tree*. The R-node Rn_1 points to its child node Rn_2 containing five records (from $C-value_{ch_1}$ to $C-value_{ch_5}$). Here we use $C-value_p$ and $C-value_{ch}$ to denote the parent product category and the child product category, respectively. $[10, 60]$ is the transaction amount range, and $[1, 5]$ is transaction time range. 32 is the total number of

transactions in the current product category represented by $C-value_p$.

When a new record $\langle C-value_{ch_6}, [15, 15], [6, 6], 1 \rangle$ (i.e., a new product category) is inserted to the R-node Rn_2 , it overflows, and then this record is moved to a new R-node Rn_3 . Meanwhile, Rn_3 is pointed to by another new record generated in Rn_1 , and the data fields $[ta_{min}, ta_{max}]$, $[t_{min}, t_{max}]$, $count_r$ and sum_r in this record are updated to reflect the ranges and aggregates of its child node (see Fig. 13(a)).

The split of either an L-node or an I-node that occurs in an *MK-tree* is more complicated, and includes two situations, respectively.

1) L-node split

Situation 1: If the record to be inserted in an L-node has the same transaction time (i.e., x-coordinate) as a record existing in that L-node, the L-node splits according to the transaction amounts of all the records it contains.

Fig. 13(b) illustrates the split of an L-node Ln_1 after inserting a new record $\langle 30, 2, 1 \rangle$, which leads to a new L-I-node $In(L)_1$. The number 30 is the *transaction amount*, 2 is the *transaction time* and 1 is the field $count_r$ in sequence. Note that the inserted record first needs to be checked whether the transactions with the same price selling the same product have already been indexed by the records in Ln_1 . If there exists repeated transactions, instead of splitting the L-node Ln_1 , we only update $count_r$ and sum_r in the corresponding record within Ln_1 . For the L-I-node $In(L)_1$, in order to get the full partition on the entire transaction amount space, the boundary is set to the intermediate value of the maximal transaction amount in the generated new L-node Ln_1 and the minimal transaction amount in the L-node Ln_2 . For instance, in Fig. 11(b), the y-coordinate of a boundary K_1K_2 equals to $\lfloor \frac{y_{\beta_2} + y_{\beta_3}}{2} \rfloor$. Hence, the two records in a generated L-I-node $In(L)_1$ are $\langle [0, 13], [1, 2], 0, Q_1 \rangle$ and $\langle [13, \infty), [1, 2], 0, Q_2 \rangle$, where Q_1 and Q_2 point to an aB^+ -tree, respectively.

- **aB^+ -tree split:** When an L-node pointed by a record in the L-I-node is split into two L-nodes, correspondingly, the aB^+ -tree pointed by this record also needs to be split. For example, we assume that all the transactions represented by the points in Fig. 11(b) are in the same brand-based product category. If the rectangle $b_1b_2b_3b_4$ splits into two rectangles $b_1K_1K_2b_4$ and $K_1b_2b_3K_2$, the original aB^+ -tree splits into two aB^+ -trees that store the information of one point (i.e., α_1) and two points (i.e., α_2, α_3) in $a_1a_2a_3a_4$, respectively.

Figure 13: The construction of a CMK-tree

Situation 2: If the record to be inserted in an L-node has a different transaction time (i.e., x-coordinate), a new L-node is generated for it.

Fig. 13(c) illustrates that if the record inserted to the L-node Ln_1 is $\langle 30, 3, 1 \rangle$, a new L-node Ln_2 is generated. Meanwhile, an L-I-node $In(L)_1$ is generated with two records pointing to Ln_1 and Ln_2 . The two records in the I-node $In(L)_1$ are $\langle [1, 15], [1, 3], 0, Q_1 \rangle$ and $\langle [0, \infty), [3, \infty), 9, Q_2 \rangle$.

- **Generate a new aB^+ -tree:** In Fig. 13(c), the record $\langle [0, \infty), [3, \infty), 9, Q_2 \rangle$ in the I-node $In(L)_1$ surrounds a new rectangle. Accordingly, a new aB^+ -tree pointed by Q_2 has to be generated to index the transactions in the same brand-based product category whose generated intervals along Transaction Time dimension intersect with the left border 3 : $[0, \infty)$. In

addition, the number 9 (i.e. *count_r*) denotes the total number of such transactions.

In Fig. 13(c), we assume that two records $\langle 5, 1, 1 \rangle$ and $\langle 5, 2, 2 \rangle$ in the L-node Ln_1 index the transactions selling the same product but traded at different time; another two records $\langle 15, 1, 1 \rangle$ and $\langle 15, 2, 3 \rangle$ index the transactions selling different products but traded at the same price. The new aB^+ -tree pointed by Q_2 is equivalent to the aB^+ -tree pointed by Q_1 after inserting four different records: $\langle 5, 3 \rangle$, $\langle 10, 2 \rangle$, $\langle 15, 1 \rangle$ and $\langle 15, 3 \rangle$. However, since the record $\langle [1, 15], [1, 3], 0, Q_1 \rangle$ in the I-node $In(L)_1$ represents the initial rectangle, the aB^+ -tree pointed by Q_1 is null in this example and the field *count_r* is 0. Here the above four records do not include the Transaction Time dimension, as each aB^+ -tree is built in a separate transaction amount dimension. The insertion and split of an aB^+ -tree are the same as those of a B^+ -tree [3].

Notice that 3 in the record $\langle 5, 3 \rangle$ is the aggregated value for the field of $count_r$ in two records $\langle 5, 1, 1 \rangle$ and $\langle 5, 2, 2 \rangle$, as they index the transactions selling the same product. Also, the records $\langle 15, 1 \rangle$ and $\langle 15, 3 \rangle$ index the transactions selling different products and thus they should be inserted separately.

- **Merge aB^+ -trees:** Several aB^+ -trees may need to be merged to generate a new aB^+ -tree. In Fig. 13(b), assume another record $\langle [0, \infty), [3, \infty), 10, Q_3 \rangle$ is to be inserted in the L-I-node $In(L)_1$. Since two records $\langle [0, 13], [1, 2], 0, Q_1 \rangle$ and $\langle [13, \infty), [1, 2], 0, Q_2 \rangle$ in the original L-I-node $In(L)_1$ have the same time range $[1, 2]$, the two aB^+ -trees pointed by Q_1 and Q_2 respectively first need to be merged to form a new aB^+ -tree. Then, the newly generated aB^+ -tree is pointed by Q_3 . The above operations are performed on all the records with the same time range.

Here we need to emphasize that since the L-node split in Situation 2 leads to the problem of space utilization, in order to guarantee the minimum space utilization for each L-node larger than 50%, Situation 2 happens only when all the L-nodes are at least half full.

2) I-node split

Situation 1: If the record to be inserted in an I-node has the same transaction time range as an existing record in that I-node, all the records with the same transaction time range as the inserted record will be moved to a newly generated I-node. In addition, if each record in an I-node has the same transaction time range as the inserted record, the same as the L-node split in Situation 1, the I-node splits according to the transaction amount ranges of all the records it contains.

In Fig. 13(d), for example, if the record $\langle [15, 30], [3, \infty), 9, Q_5 \rangle$ in the L-I-node $In(L)_1$ splits into two new records $\langle [15, 20], [3, \infty), 5, Q_5 \rangle$ and $\langle [20, \infty), [3, \infty), 4, Q_6 \rangle$, the above two records lead to the overflow of $In(L)_1$. Then, the node $In(L)_1$ will continue to split into two L-I-nodes: a new $In(L)_1$ and a new $In(L)_2$. Meanwhile, another I-I-node $In(I)_3$ with two records $\langle [0, 50], [1, 3], 0 \rangle$ and $\langle [0, \infty), [3, \infty), 19 \rangle$ ($19 = 10 + 9 = 10 + 5 + 4$) is generated to point to the node $In(L)_1$ and the node $In(L)_2$, respectively.

Situation 2: If the record to be inserted in an I-node has a different transaction time range, similar to the L-node split in Situation 2, a new I-node is generated to contain the inserted record. Such a strategy is to guarantee the maximum space utilization for an I-node.

In Fig. 13(e), if the record $\langle [0, \infty), [4, \infty), 19 \rangle$ is inserted to $In(L)_1$, a new L-I-node $In(L)_2$ is generated. Meanwhile, an I-I-node $In(I)_3$ with two records $\langle [0, 50], [1, 4], 0 \rangle$ and $\langle [0, \infty), [4, \infty), 19 \rangle$ is generated to point to the I-nodes $In(L)_1$ and $In(L)_2$, respectively. Notice that each record in node $In(I)_3$ will not include a pointer Q_i so as to avoid duplication of the aB^+ -tree. This is because the same aB^+ -tree can already be indexed by its child node $In(L)_2$, which is an L-I-node.

Algorithm 1 presents pseudo-code for the complete insertion process.

6.3 CTT Computation Algorithm

Basically, the CTT computation algorithm answers a typical buyer's CTT queries covering three transaction dimensions based on our proposed *CMK-tree*. The processing of

ALGORITHM 1: The CMK-tree Construction

Input: A transaction TR_i includes $C-hrchy_i$, ta_i , t_i and r_i .
Output: CMK-tree

- 1: // construct a *C-tree*
- 2: Starting from the “Root” of the product category hierarchy
- 3: Determine the path in *C-tree* based on the $C-hrchy_i$ of each transaction TR_i .
- 4: **for all** R-nodes along the path **do**
- 5: **if** The product traded in TR_i belongs to a new product category on which the seller has no prior transactions **then**
- 6: i. insert the generated new record in corresponding R-node.
- 7: ii. **if** the R-node overflows, split.
- 8: **else**
- 9: update corresponding ranges and aggregates maintained in a record
- 10: **end if**
- 11: **end for**
- 12: // construct the *MK-trees* that are external to the *C-tree*
- 13: **for all** L-nodes and I-nodes in the path from bottom up **do**
- 14: **if** the node is the L-node **then**
- 15: i. **if** transaction time t_i is different from any transactions in the L-node, and this L-node is at least half full, then generate a new L-node.
- 16: ii. **if** transaction time t_i is the same as a record in the L-node, and repeated transactions have already been indexed in this L-node, then update corresponding $count_r$ and sum_r .
- 17: iii. otherwise, insert the transaction TR_i
- 18: iv. **if** the L-node overflows, split
- 19: **else if** the node is the I-node **then**
- 20: i. insert the generated new records
- 21: ii. **if** the I-node overflows, split
- 22: **end if**
- 23: **end for**

CTT computation starts by locating product category in the *C-tree* according to the *C-value* (i.e. product category) in a buyer's query. Then, it computes the left border VRA and the right border VRA (see Fig 3(b)) in one or several *MK-trees*, respectively, depending on the number of brand-based product categories that are included in a CTT query.

For example, to answer a typical CTT query: $\langle \text{product-category: “Audio device”, price-range: “\$100-\$200”, time-range: “the latest 6 months”} \rangle$, all the sub-categories of the product category specified in a CTT query are first considered (see Fig. 8). As each record in an R-node contains a transaction amount range ($[ta_{min}, ta_{max}]$) and a transaction time range ($[t_{min}, t_{max}]$) for its corresponding product category, there are three cases that should be differentiated.

Case 1: If a CTT query on the transaction amount range and the transaction time range falls into the region surrounded by $[ta_{min}, ta_{max}]$ and $[t_{min}, t_{max}]$, then it is not necessary to search its child node (sub-categories). Instead, $count_r$ and sum_r in that record can be used directly.

Case 2: If a CTT query on the transaction amount range and the transaction time range are outside the region defined by $[ta_{min}, ta_{max}]$ and $[t_{min}, t_{max}]$, then it is not necessary to search its child node (sub-categories) either.

Case 3: If a CTT query on the transaction amount range and the transaction time range overlaps with the region surrounded by $[ta_{min}, ta_{max}]$ and $[t_{min}, t_{max}]$, then the search iteratively executes from Case 1 to Case 3 in its descendants until reaching the layer of I-nodes. Taking each reached I-node as the root of an *MK-tree*,

all the corresponding MK-trees are searched for the left border VRA and the right border VRA, respectively.

For *Case 3*, we take the computation of a VRA 2 : $[0, 5]$ as an example to introduce the search process in an MK-tree. As depicted in Fig. 13(d), the I-nodes, the rectangle represented by which contains 2 : $[0, 5]$, are iteratively searched until reaching the layer of L-I-nodes, and thus the record $\langle [0, 13], [1, 3], 0, Q_1 \rangle$ in the L-I-node $In(L)_1$ is selected. In order to compute the VRA 2 : $[0, 5]$, both the aB^+ -tree and the L-node pointed by the above record need to be searched, and the VRA equals to the sum of the two search results. Note that instead of visiting only one record as introduced in the above example, the search for computing the VRA may be executed on several aB^+ -trees as well as L-nodes pointed by the corresponding records, respectively, depending on the number of the rectangles overlapped by the query range in the transaction amount dimension. For instance, to compute another VRA 3 : $[10, 30]$ based on Fig. 13(d), two records $\langle [0, 15], [3, \infty), 10, Q_4 \rangle$ and $\langle [20, \infty), [3, \infty), 4, Q_6 \rangle$ in the L-I-node $In(L)_2$ are selected for conducting the further searches. The aggregation results ($count_r$ and sum_r) in the record $\langle [15, 20], [3, \infty), 4, Q_5 \rangle$ can be used directly, as the transaction amount range $[15, 20]$ in that record falls inside the query range $[10, 30]$ in the transaction amount dimension.

If the transaction time for a VRA equals to the left border of a rectangle represented by the selected record in an L-I-node, search only performs on the aB^+ -tree pointed by this record. For example, in Fig. 13(e), to compute the VRA 3 : $[5, 10]$, the record $\langle [0, 15], [3, 4], 10, Q_4 \rangle$ in the L-I-node $In(L)_1$ is selected. Instead of searching L-node, only the aB^+ -tree pointed by the above record is searched. However, since the right border in CTT computation is always fixed to the point “now”, the search for computing the right border VRA is performed on both the aB^+ -trees and L-nodes pointed by the selected records.

Algorithm 2 describes the process of CTT computation in a CMK-tree.

6.4 Structure and Performance Analysis

In this section, we will provide an analytical study on the CMK-tree, focusing on its structure and query performance. The symbols and their meanings used in our analysis are explained in Table 1.

Property 1. *Each MK-tree in a CMK-tree represents a two-dimensional space formed by transaction amount and transaction time for all the transactions in a brand-based product category. All the records in each layer of I-nodes in an MK-tree fully partition the corresponding two-dimensional space into multiple nonintersecting rectangles*

Assume all the transactions in a brand-based product category are represented by a number of points in two-dimensional space depicted in Fig. 11(a). Since the insertions come in the nondecreasing time order, a new insertion only happens in the latest version of “domain 0” K-D-B-tree, for example, the version 3 in Fig. 11(a). Meanwhile, the division within each version can only be operated along the transaction amount dimension (y-axis). As shown in Fig. 13(b) and Fig. 13(c), each record in an L-I-node corresponds to either a generated new version for “domain 0” K-D-B-tree (e.g., $\langle [0, \infty), [3, \infty), 9, Q_2 \rangle$) or a partition in the latest version (e.g., $\langle [0, 13], [1, 2], 0, Q_1 \rangle$). Obviously,

ALGORITHM 2: CTT Computation Algorithm in a CMK-tree

Input: A typical CTT query with specific product category, transaction amount range $([ta_1, ta_2])$ and transaction time range $([t_1, t_2])$.
Output: CTT value

- 1: CTT=0
- 2: $count_{r1}=0, sum_{r1}=0, count_{r2}=0, sum_{r2}=0$
- 3: The Searching starts from the “Root” of product category hierarchy
- 4: Determine the layer in product category hierarchy based on the CTT query on product category, and return corresponding record R in an R-node.
- 5: begin Search(CMK-tree, R)
- 6: if the record is in an R-node then
- 7: **Case 1:** CTT=CTT+ $\frac{sum_{r1}}{count_{r1}}$, $count_{r1}$ and sum_{r1} are from the record
- 8: **Case 2:** CTT=CTT
- 9: **Case 3:** Search(CMK-tree, $R_{childnode}$)
- 10: else if the record is in an I-node then
- 11: Let rec_1 be the index record whose rectangle contains $t_1 : [ta_1, ta_2]$ // for the left border VRA
- 12: Let rec_2 be the index record whose rectangle contains $t_2 : [ta_1, ta_2]$ // for the right border VRA
- 13: while neither rec_1 nor rec_2 is a record in L-I-nodes do
- 14: i. rec_1 be its child whose rectangle contains $t_1 : [ta_1, ta_2]$
- 15: ii. rec_2 be its child whose rectangle contains $t_2 : [ta_1, ta_2]$
- 16: end while
- 17: for all rec_1 s do
- 18: if t_1 equals to the left border of rec_1 then
- 19: only search aB^+ -tree that is pointed by rec_1 for left border to aggregate $count_{r1}$ and sum_{r1}
- 20: else
- 21: the search conducts on both the aB^+ -tree and the L-node pointed by rec_1 to aggregate $count_{r1}$ and sum_{r1}
- 22: end if
- 23: end for
- 24: for all rec_2 s do
- 25: the search conducts on both aB^+ -tree and L-node pointed by rec_2 to aggregate $count_{r2}$ and sum_{r2}
- 26: end for
- 27: CTT=CTT+ $\frac{sum_{r2}-sum_{r1}}{count_{r2}-count_{r1}}$
- 28: end if
- 29: end Search

these records partition the complete two-dimensional space. More importantly, the rectangles formed by them are nonintersecting. In addition, except for the records in L-I-nodes, the records in I-I-nodes (a higher level) still fully partition two-dimensional space into multiple nonintersecting rectangles, for example, the records in node $In(I)_3$ depicted in Fig. 13(d) and Fig. 13(e).

Property 2. *To answer a CTT query for each brand-based product category, the CMK-tree guarantees almost linear query performance*

Now, let us refer to the CTT computation algorithm given in Section 6.3, the method of computing the left border VRA and the right border VRA is adopted while answering a CTT query. In order to clearly understand property 2, we first examine the performance of computing each VRA. Property 1 has illustrated that the transaction amount ranges and transaction time ranges of the records in the I-nodes in an MK-tree do not intersect each other. Thus, when computing a VRA, the search traverses from top to bottom in an MK-tree until reaching the layer of L-I-nodes. Then, one or several corresponding records in L-I-nodes are chosen. Finally, both the aB^+ -trees and the leaf nodes pointed to by these records are searched. To sum up, the structure of MK-tree achieves logarithmic time cost ($O(\log n)$) for computing each VRA. Hence, to answer a buyer’s CTT queries for a specific

Table 1: List of symbols

symbol	explanation
S	a seller
$Trans$	the transaction dataset for the seller S
n	the number of past transactions contained in $Trans$
m	the number of brand-based product categories (see Fig. 7) to which n past transactions belong
n_i	the number of points in a two-dimensional space formed by the transactions in a brand-based product category.
h	the height of the product category hierarchy for a newly happened transaction
n_h	the number of points in a two-dimensional space formed by the transactions in $Trans$ which are in the same brand-based product category as the newly happened transaction
nc_L	the capacity of an L-node in a <i>CMK-tree</i>
nc_I	the capacity of an I-node in a <i>CMK-tree</i>

m : The number of brand-based product category determines the size of *C-tree*.

n_i : For m brand-based product categories, we have $\sum_{i=1}^m n_i \leq n$. This is because one point may represent a set of repeated transactions that occurred on a day (see *Case 2* in Section 5). In practice, $\sum_{i=1}^m n_i$ may be much less than n .

nc_I : The difference of node capacity between I-I-node and L-I-node is ignored in our discussion.

brand-based product category, the query of *CMK-tree* is almost linear. Also, this property will be demonstrated in the experiments to be introduced in Section 8.

When a buyer performs “roll up” operations, the search will be iteratively executed from *Case 1* to *Case 3* mentioned in Section 6.3 in the descendants of current R-node, and finally one or several *MK-trees* are selected. The search then continues in the selected *MK-trees* twice for computing the left VRA and the right border VRA, respectively. Note that the number of *MK-trees* may be much less than m in practice. Therefore, we have linearithmic time cost ($O(n \log n)$) in total. However, the *CMR-tree* has better performance than all the existing approaches that were proposed in [61] (see Section 8). This is a significant advantage in answering CTT queries.

Next, we analyse the space utilization of the *CMK-tree* that is important to evaluate disk-based index schemes. We adopt the same analysis method as in [17] and consider the predictability of space utilization, i.e. minimum space utilization of each node.

Lemma 1. *The minimum space utilization is no less than $\frac{nc_L}{2}$ for an L-node; The minimum space utilization is no less than $\frac{nc_I}{3}$ on average for an I-node.*

PROOF. Let t_1, t_2 and t_3 be three different time periods. Suppose an initial state that all the records in the L-node Ln_1 have the same transaction time t_1 . For a new record with the transaction time t_2 to be inserted in Ln_1 , there are two cases. (1) If space utilization of Ln_1 is no less than $\frac{nc_L}{2}$, a new L-node Ln_2 is established. (2) Otherwise, the new record with the transaction time t_2 is inserted into Ln_1 until it overflows. Then, the node Ln_1 splits into a new Ln_1 and a new L-node Ln_2 . The space utilization of each generated L-node is still no less than $\frac{nc_L}{2}$. All the records in the two L-nodes are within the same time range $[t_1, t_2]$. In this case, if the new records with the transaction time t_2 continue to be inserted in an L-node, either Ln_1 or Ln_2 is selected as the targeted L-node depending on the transaction amount of the new record. Note that both Ln_1 and Ln_2 might split again during insertion, but the minimum space of any generated new L-nodes is no less than $\frac{nc_L}{2}$, and the records maintained in each node are within a time range $[t_1, t_2]$. The above operations will be repeated until a record with the transaction time t_3 is inserted. This is because a

new L-node is established for that record. So, the minimum space utilization is no less than $\frac{nc_L}{2}$ for an L-node. In fact, according to our analysis, except for the L-nodes with the minimum space utilization no less than $\frac{nc_L}{2}$, there is at most one L-node with space utilization less than $\frac{nc_L}{2}$. In particular, this specific L-node includes the records that are most recently inserted. For example, the newly generated L-node maintains only one record with the transaction time t_3 .

To estimate the space utilization of I-nodes, we consider the worst case. Let t_1, t_2, t_3 and t_4 be four different time periods. Still, we suppose an initial state that a full I-node In_1 with nc_I records includes only one record with the transaction time range $[t_1, t_2]$. The rest of the records in In_1 have the same transaction time range $[t_3, t_4]$. If a new record with a transaction time range $[t_3, t_4]$ to be inserted in the I-node In_1 , the node In_1 overflows. Then, it splits into a new In_1 maintaining the one record with the transaction time range $[t_1, t_2]$ and another full I-node Ln_2 . All the records in node Ln_2 have the same time range $[t_3, t_4]$. In such a case, if a new record with the transaction time range $[t_3, t_4]$ continues to be inserted in an I-node, the node Ln_2 is selected as the targeted I-node. Then, the node In_2 overflows and splits into two I-nodes according to the transaction amount ranges of all the records it contains. Hence, due to continuous splits of I-nodes, the records in the original full I-node In_1 are distributed in three different I-nodes. We conclude that, in the worst case, the minimum space utilization is no less than $\frac{nc_I}{3}$ on average for an I-node. \square

Lemma 2. *The height of an MK-tree in the CMK-tree is at most $\lceil \log_{\lceil \frac{nc_I}{3} \rceil} \lceil \frac{n_i}{\lceil \frac{nc_L}{2} \rceil} \rceil \rceil + 1$ ($\forall i \in [1, m]$). The number of aB^+ -trees in the CMK-tree pointed by L-I-nodes is at most $\sum_{i=1}^m \lceil \frac{n_i}{\lceil \frac{nc_L}{2} \rceil} \rceil$.*

PROOF. First, we examine the height of an *MK-tree* that is built based on the transactions in a brand-based product category. For m *MK-trees* in a *CMK-tree*, we focus on analyzing one of them. Suppose the past transactions in a brand-based product category form n_i ($\forall i \in [1, m]$) points in a two-dimensional space. In Lemma 1, we have proved that the minimum space utilization is no less than $\frac{nc_L}{2}$ for an L-node. In addition, there may exist one L-node with space utilization less than $\frac{nc_L}{2}$. Hence, the number of L-nodes in

an *MK-tree* is at most $\lfloor \frac{n_i}{\lfloor \frac{nc_L}{2} \rfloor} \rfloor$. The above L-nodes will be indexed by I-nodes, each of which has the minimum space utilization no less than $\frac{nc_L}{3}$ on average. Hence, the height

of an *MK-tree* in the *CMK-tree* is at most $\lceil \log_{\lfloor \frac{nc_L}{3} \rfloor} \lfloor \frac{n_i}{\lfloor \frac{nc_L}{2} \rfloor} \rfloor \rceil + 1$.

Since the number of transactions traded by the seller S in m brand-based product categories has an imbalanced distribution, each *MK-tree* has a different height. The *CMK-tree* is an unbalanced tree.

Second, we examine the total number of aB^+ -trees, each of which is pointed by a record in an L-I-node. There are at most $\lfloor \frac{n_i}{\lfloor \frac{nc_L}{2} \rfloor} \rfloor$ L-nodes in an *MK-tree*, and each L-node is pointed by a record in an L-I-node. So, the number of aB^+ -trees in an *MK-tree* is also $\lfloor \frac{n_i}{\lfloor \frac{nc_L}{2} \rfloor} \rfloor$ at most. Therefore, for m *MK-trees* in the *CMK-tree*, the total number of aB^+ -trees is at most $\sum_{i=1}^m \lfloor \frac{n_i}{\lfloor \frac{nc_L}{2} \rfloor} \rfloor$. \square

Theorem 1. In a *CMK-tree*, the number of nodes accessed for an insertion operation is $O(h) + O(\log_{\frac{nc_L}{3}} \frac{n_h}{nc_L}) + 1$.

PROOF. For an insertion operation in the *CMR-tree*, we consider the insertion cost in the worst case. As described in Section 6.2.1, an insertion operation first searches a path in the *C-tree* based on the *C-hrchy* of the newly happened transaction. The number of accessed nodes is $O(h)$. Then, the insertion operation traverses an *MK-tree*. Lemma 2 illustrates that the height of an *MK-tree* in the *CMK-tree* is at most $\lceil \log_{\lfloor \frac{nc_L}{3} \rfloor} \lfloor \frac{n_i}{\lfloor \frac{nc_L}{2} \rfloor} \rfloor \rceil + 1$ ($\forall i \in [1, m]$). Hence, the number of accessed nodes for inserting a newly happened transaction in an *MK-tree* is $O(\log_{\frac{nc_L}{3}} \frac{n_h}{nc_L}) + 1$. As a result, the total number of accessed nodes is $O(h) + O(\log_{\frac{nc_L}{3}} \frac{n_h}{nc_L}) + 1$ for an insertion operation. \square

7. CMR-TREE^{RS}—THE CMK-TREE WITH REDUCED STORAGE SPACE

In the *CMK-tree*, transaction data and ratings are aggregated at the granularity of a day. Though it consumes smaller storage space than the actual data, with significant increase of historical transaction data, the size of the *CMK-tree* will become much larger. In this section, we introduce a new approach *CMK-tree*^{RS}, which reduces storage space consumption for a *CMK-tree*, and offers great benefit to the trust management system with millions of sellers.

In Section 2.4, we have pointed out that the Hierarchical Temporal Aggregation model with fixed storage space (*HTA*^{FS}) [53] can be applied to CTT computation, in order to control the size of the storage space allocated to a seller for storing aggregation index [57]. However, as a matter of fact, it is difficult to select the size of the fixed storage space, since the number of distinct products as well as the number of product categories in the transactions traded by different sellers are different. Now let us consider an example. Assume two sellers S_1 and S_2 have the same volume of transaction data over a period of time. The transactions traded by S_1 are widely distributed in multiple product categories, but seller S_2 has numerous repeated transactions belonging to only a few product categories. For S_1 , it is necessary to allocate a relatively large storage space to store

aggregation index so as to obtain his/her trust level in each product category and a corresponding sub-category. In contrast, for S_2 , it is not necessary to allocate the storage space with the same size as S_1 , because most transactions are repeated, leading to less storage space consumption for storing aggregation index.

In practice, the time range in CTT queries is usually “the latest 1 month”, “the latest 3 months”, “the latest 6 months”, or “the latest 12 months”. When adopting a *CMK-tree* for CTT computation, the above time ranges can be searched, but the *CMK-tree* consumes a large storage space as the aggregation granularity in the Transaction Time dimension is “a day”. Alternatively, if we aggregate ratings at a coarse time granularity of a month, as depicted in Fig. 11(a), the number of points in a two-dimensional space formed by transactions further decreases, since more repeated transactions exist in a month than a day. In such a case, the size of storage space consumed for a *CMK-tree* can be reduced to a large extent. However, such a coarse aggregation granularity leads to a serious problem regarding the accuracy of CTT computation. For instance, if the current time is “August 10”, to answer a buyer’s CTT query with the specified time range as “the latest 1 month”, the result can be computed based on either the data of “August” only or the data of both “August” and “July”. However, either way can not guarantee the accuracy of CTT results. In the worst case, the ratings for computing a CTT value of “the latest 1 month” come from one day only or one month plus 29 days (if one month contains 30 days). On average, the CTT result comes from the ratings of 1 month $\pm \frac{1}{2}$ month.

In the proposed approach *CMK-tree*^{RS}, a new strategy is adopted, which aggregates ratings with different time granularities for different time periods. In other words, in the *CMK-tree*^{RS}, the ratings within the latest t days are aggregated at a fine time granularity of a day, and the ratings of t days ago are aggregated at a coarse time granularity of a week. Taking into account the problem of accuracy of CTT values as mentioned in the above, our work provides a tradeoff between storage space consumption and accuracy. In addition, in practice, t is set to be 90 days. Therefore, for CTT queries regarding a seller’s trust level of “the latest 1 month” or “the latest 3 months”, there is no accuracy problem in the time dimension. For the queries of “the latest 6 months”, on average, ratings included in computation cover 6 months $\pm \frac{1}{2}$ week. Likewise, in the case of “the latest 12 months”, on average, the ratings used in CTT computation cover 12 months $\pm \frac{1}{2}$ week.

7.1 Construction of the *CMK-tree*^{RS}

This section describes the process of *CMK-tree*^{RS} construction. The algorithm for *CMK-tree*^{RS} construction adds the following operations to Algorithm 1, which is given in Section 6.2 and is used for building a *CMK-tree*:

- If $t_{now} - t_{begin} \leq t + 1$, insert the data of a newly happened transaction into the initial *CMK-tree* based on Algorithm 1. The term t_{begin} denotes the starting time and the term t_{now} denotes the current time. As new transactions happen everyday, in order to guarantee the ratings within the latest t days to be aggregated at a fine time granularity, firstly, it is necessary to perform insertion operations leading to the aggregations of $t + 1$ days. Then, the ratings of t days ago are moved

Figure 14: The general structure of the $CMK-tree^{RS}$

with the same x-coordinate. As stated before, the standardization operation essentially leads to a smaller size for the $CMK-tree^{RS}$. In Section 7.2, we will further explain how and why the $CMK-tree^{RS}$ can also reduce the time of computing CTT values.

- Generate the second $MK-tree$, namely $MK-tree^{week}$, using the standardized results. Consequently, instead of having only one $MK-tree$, each subtree that is external to the $C-tree$ has both an $MK-tree^{day}$ and an $MK-tree^{week}$ in the new $CMK-tree^{RS}$. Fig. 14 illustrates the general structure of the $CMK-tree^{RS}$. Note that if there already exist two $MK-trees$ with aggregation index at different time granularities in an external subtree, the $MK-tree^{week}$ is updated by inserting the standardized results.

7.2 CTT computation based on the $CMK-tree^{RS}$

When answering a CTT query based on the new structure $CMK-tree^{RS}$, like Algorithm 2 given in Section 6.3, the $C-tree$ is first searched. Then, it computes the left border VRA and the right border VRA in the subtrees that are external to the $C-tree$. Moreover, each external subtree in $CMK-tree^{RS}$ has up to two $MK-trees$ with aggregated ratings at different time granularities (see Fig. 14). Therefore, the computation of the left border VRA and the right border VRA may also be performed in $MK-tree^{day}$ and $MK-tree^{week}$ respectively, depending on the query range in the Transaction Time dimension. If the specified time range in a CTT query is $[t_{now} - t, t_{now})$, only the $MK-tree^{day}$ is searched; otherwise, the CTT computation algorithm searches both the $MK-tree^{day}$ and the $MK-tree^{week}$ in the corresponding external subtrees.

Now we introduce an example for further explanation. Suppose that the current time refers to the day of “July 20” and t is set to 90 days. For an external subtree in the $CMK-tree^{RS}$ that includes two $MK-trees$, the $MK-tree^{day}$ maintains the aggregated ratings with the time range [April 21, July 20) and the $MK-tree^{week}$ maintains the aggregated ratings with the time range [January 1, April 21). In this case, if a buyer’s CTT query has “the latest 6 months” as the time range, the search for computing the left border VRA is performed on the $MK-tree^{week}$. In contrast, for a $CMK-tree$ with an $MK-tree$ as each external subtree, the $MK-tree$ maintains the aggregated ratings for around 200 days in total (i.e. from January 1 to July 20) with the time granularity of days. Though the $CMK-tree^{RS}$ has two subtrees: $MK-tree^{day}$ and $MK-tree^{week}$, they are much smaller

in size. On one hand, the $MK-tree^{day}$ includes the aggregates of ratings in a short period of time (i.e. 90 days *vs* 200 days). On the other hand, the $MK-tree^{week}$ stores the aggregations for the remaining period of time at a coarse time granularity of “a week” rather than “a day”. Therefore, based on the $CMK-tree^{RS}$, the time of computing both the left border VRA and the right border VRA can be reduced. The experiment results to be introduced in Section 8 also have illustrated the performance improvement of the $CMK-tree^{RS}$ in answering buyers’ CTT queries.

8. EXPERIMENTS

In this section, we introduce the results of the experiments conducted on four large datasets, which compares the proposed $CMK-tree$ and $CMK-tree^{RS}$ with three existing approaches $eaR-tree$, $eaP-tree$ and $eH-tree$ [61] in terms of efficiency in CTT computation and storage space consumption.

Note that the effectiveness of our proposed trust vector based framework has already been studied both analytically and empirically in the earlier version of our work [60]. In particular, the trust vector based approach can reflect a seller’s dynamical trust levels in different transaction contexts and identify risks potentially existing in a forthcoming transaction, thus outperforming single-value trust valuation methods [33, 48] and prior trust vector based approach [43]. However, as mentioned at the beginning of this article, a popular seller usually has a large amount of transactions, and the transactions of such seller may be widely distributed in multiple product categories. It is very likely for many buyers to access various CTT values of the seller simultaneously. Therefore, efficient CTT computation for delivering prompt responses to a buyer’s CTT requests becomes an extremely important concern. Meanwhile, storage space consumption is also a very important aspect that should be taken into consideration.

The *ReputationPro* model proposed in this article aims to support efficient CTT computation as well as the reduction of storage space consumption with new data structures and novel algorithms. Our experiments have two parts: While Section 8.3 compares the $CMK-tree$ with the $eaR-tree$, the $eaP-tree$ and the $eH-tree$ in the computation time of CTT values, Section 8.4 further compares the $CMK-tree$ and the $CMK-tree^{RS}$ in the aspects of both CTT values computation time and space consumption.

8.1 Datasets

8.1.1 eBay Datasets

With eBay APIs⁹, we have obtained detailed feedback and transaction data for up to 90 days of selected sellers. In seller selection, we first chose many popular products, and the sellers selling them with the largest number of reviews. With them, we finally selected two sellers S_1 and S_2 who had totally around 12,000 transactions (approx. 133 transactions per day) and 4,000 transactions (approx. 44 transactions per day) respectively within 90 days.

The products sold by S_1 and S_2 exist in multiple product categories, while most products are in the category ‘*Information, Communication and Media technology*’ (see Fig. 7). Specifically, the products sold by S_1 include *MP3 players*,

Notebooks, *Digital Cameras*, *CD & DVD player*, *LCD monitors* etc, and the products sold by S_2 include *Digital Cameras*, *Video Cameras*, *Camera & Photo Accessories*, *Printers*, *Smartphones* etc. Note that the categories are descendingly ordered according to the volume of transactions. The selection of S_1 and S_2 allows performing both “drill down” and “roll up” operations in the product category hierarchy (see Fig. 7) when doing finer-grained analysis on a seller’s transaction reputation.

8.1.2 Four Large Synthetic Datasets

Considering that only 90 days transaction data of a seller can be obtained from eBay, and the time range in a CTT query can be “*the latest 6 months*” or “*the latest 12 months*”, we generated four large synthetic datasets $SD_1(S_1)$, $SD_2(S_1)$, $SD_3(S_2)$ and $SD_4(S_2)$ based on the transaction data of eBay sellers S_1 and S_2 . In each synthetic dataset, we expanded the time period of transactions and the daily volume of transactions so as to test the performance of our proposed approaches under the circumstances with exceptionally large volumes of transactions. Specifically, the above four synthetic datasets are further categorized into two types.

(1) Type I includes $SD_1(S_1)$ for S_1 and $SD_3(S_2)$ for S_2 : To generate the two datasets, we duplicated the transaction data of each seller 10 times on a given day, and then duplicated the transactions data of 90 days to form the transaction data of 12 months. Thus, two datasets contain about 480,000 and 160,000 transactions in total (i.e., approx. 1330 transactions per day for S_1 and 440 transactions per day for S_2), respectively. Type I synthetic datasets guarantee that the proportion of each sold product is the same on a daily basis in both the synthetic dataset and the corresponding real dataset.

(2) Type II includes $SD_2(S_1)$ for S_1 and $SD_4(S_2)$ for S_2 : Each dataset contains transaction data 10 times as much as that of the seller on a given day, and contains transaction data for 12 months totally. In each Type II synthetic dataset, a transaction is randomly selected from the corresponding seller’s eBay real dataset. In Type II synthetic datasets, any product appears in the corresponding real dataset. But the proportion of it on a day or a month is different to that in the real dataset.

8.2 Experiment Setup

The parameters used in the experiments are as follows: the same page size of 1KB applies to all five index schemes; it is 4 bytes for each of the transaction amount, transaction time, $count_x$ and sum_x in a record and the C -value is of 8 bytes; t in the $CMK-tree^{RS}$ is set to be 90 days, namely, the ratings within the latest 90 days are aggregated at a fine time granularity by days, and the ratings of 90 days ago are aggregated at a coarse time granularity by weeks. In addition, each approach is implemented using VC++ 6.0 running on a Lenovo Y560 laptop with an Intel Core i5 CPU (2.20GHz), 2GB RAM, Windows 7 Professional operation system and MySQL 5.1.35 relational database.

To evaluate the CTT query performance, we measure the CTT values computation time. For each seller, we generated the corresponding queries on either *Transaction Item Specific Trust* (TIST) or *Product Category based Trust* (PCT), covering three transaction dimensions (denoted as **3D CTT queries**), and the queries on *Similar Transaction Amount*

⁹developer.ebay.com/support/docs

based *Trust* (STAT), covering two transaction dimensions (denoted as **2D CTT queries**).

To generate *3D CTT queries*, based on eBay datasets, we first selected 5 popular products traded by the sellers, each of which has two characteristics: (1) “roll up” operations can be preformed continuously at least 3 times along a path in the corresponding product category hierarchy; (2) each product category along the path contains a large number of transactions. Table 2 lists the selected products for two popular sellers. Then, we set the time range in CTT queries to be “the latest 1 month” and computed their TIST values. After that, for each of 5 selected products, “roll up” operations were performed continuously 3 times along a path in the product category hierarchy to generate the *3D queries* on PCT. To generate the price range in each PCT query, we adopted a strategy to partition the transaction amount range of the current product category that is included in a PCT query. Specifically, as each product category in the product category hierarchy maintains its corresponding transaction amount range $[ta_1, ta_2]$, we partitioned this transaction amount range into 3 equal intervals, and each interval is regarded as an input for the price range in a PCT query. Thus, each product category corresponds to 3 PCT queries with different price ranges. In total, there are 45 ($5 \times 3 \times 3$) *3D queries* on PCT values. For instance, the generated PCT queries for the product “Apple iPod nano 16GB (mc696ll/a)” sold by S_1 (see Table 2) are <product-category: “Apple MP3 player (iPod)”, price-range: “\$100-\$200”, time-range: “the latest 1 month” > (i.e. PCT at layer 5) and <product-category: “MP3 player”, price-range: “\$150-\$300”, time-range: “the latest 1 month” > (i.e. PCT at layer 4). Our experiments also tested the TIST and PCT queries at three different time ranges “the latest 3 months”, “the latest 6 months” and “the latest 12 months”, respectively. Thus, there are totally 200 (i.e. $(45 + 5) \times 4$) *3D CTT queries* tested for each seller.

To generate *2D CTT queries*, 45 different price ranges for the above PCT queries are used in generating *2D CTT queries*. Meanwhile, the experiments also tested 4 different time ranges “the latest 1 month”, “the latest 3 months”, “the latest 6 months” and “the latest 12 months”. Thus, there are totally 180 (i.e. 45×4) *2D CTT queries* tested for each seller.

8.3 The Comparison of the CMK-tree and Three Existing Approaches

This section includes the results of the comparison between the *CMK-tree* and three existing approaches *eaR-tree*, *eaP-tree* and *eH-tree* proposed in [61] in terms of CTT values computation time, storage space consumption and the time for tree construction. The experimental results are obtained from the execution on four large synthetic datasets, and the computation time in answering CTT queries is averaged the results of 5 independent runs.

Figure 15 and Figure 16 plot the CTT values computation time of the *eaR-tree*, the *eaP-tree*, the *eH-tree* and the *CMK-tree* in *3D CTT queries* and *2D CTT queries*. First of all, from Figure 15, we can observe:

(1) Compared with other approaches, the performance of the *eaR-tree* shows a different trend in CTT values computation time on both $SD_1(S_1)$ and $SD_2(S_1)$. When the time range in a CTT query becomes larger, it means a larger query region for the *eaR-tree*, and the computation time in-

creases almost linearly because more MBRs are overlapped by the expanded query range. In particular, if the time range in CTT queries is “the latest 12 months”, the *eaR-tree* has the worst performance in most cases.

In addition, a similar trend can be observed from the results of *eaP-tree*, *eH-tree* and *CMK-tree*, since they are all based on two VRA queries (see Section 2.3.2) to answer a CTT query. When the time range in a query expands, the computation time is stable or even in decline. In CTT queries, as the time range refers to the latest time period, the right border is always fixed to the time point “now”. Correspondingly, the time of computing the right border VRA is also fixed for *eaP-tree*, *eH-tree* and *CMK-tree*. However, when the time range in a query expands (i.e. the left border shifts to the left), the time for computing the left border VRA decreases. This is because the above three approaches take advantage of the multi-version structure (see Section 6.1.2), and the versions with their starting time later than the left border of the time range will not be visited. Note that *eaP-tree* and *eH-tree* extend a multi-version *B-tree* (MVBT) [4], and *CMK-tree* extends a multi-version “domain 0” *K-D-B-tree*. As illustrated in Figure 15 and Figure 16, if the time range in a query covers the longest time period, such as “the latest 12 months”, most versions of “domain 0” *K-D-B-trees* (see Fig. 11) have their starting time later than the left border of the time range. In such a case, only a few nodes need to be visited for computing the left border VRA. Correspondingly, the computation time for each of three approaches *eaP-tree*, *eH-tree* and *CMK-tree* drops to their minimum.

(2) The *CMK-tree* proposed in this article is superior in efficiency for computing CTT values to *eaR-tree*, *eaP-tree* and *eH-tree* on both $SD_1(S_1)$ and $SD_2(S_1)$. The *eaR-tree* extends the *aR-tree* [27], and its performance greatly depends on the regions surrounded by the transaction time range and the price range in a CTT query. The *eaP-tree*, which extends the *aP-tree* [37], indexes all transactions and cannot essentially aggregate repeated transactions, leading to inferior performance. The *eH-tree*, which improves the *eaP-tree*, is faster than the *eaP-tree* in computing CTT values. The reasons are twofold. On one hand, the *eH-tree* adopts the *aP⁺-tree* to reduce the time for computing the left border VRA. On the other hand, in *eH-tree*, the search is done in the fully ordered transaction amount space maintained in an additional *aB⁺-tree* for computing the right border VRA [61]. However, as the *eH-tree* is still based on the *eaP-tree*, it does not fundamentally resolve the problem existing in the *eaP-tree*. Moreover, from Figure 17 and Figure 18, we can see that the *eH-tree* takes longer time in constructing the aggregation index and consumes more storage space than the *eaP-tree*.

In contrast, the *CMK-tree* can not only index each specific product traded in a time period, but also aggregate repeated transactions. More importantly, it delivers fast and almost stable computation time for answering CTT queries. On average, for 200 *3D CTT queries* based on Type I synthetic dataset $SD_1(S_1)$, the *CMK-tree* reduces computation time by 33.5% of the *eaR-tree*, by 44.8% of the *eaP-tree*, and by 16.2% of the *eaH-tree*; for 180 *2D CTT queries*, the *CMK-tree* reduces computation time by 25.2% of the *eaR-tree*, by 51.5% of the *eaP-tree*, and by 18.8% of the *eaH-tree*. In addition, the improvement is more obvious on Type II synthetic dataset $SD_4(S_2)$. On average, for 200 *3D CTT*

Table 2: List of selected products from two popular sellers

seller	some selected products
S_1	<i>Apple iPod nano 16GB (mc696ll/a)</i> at a price of \$150, <i>Dell Laptop (Inspiron i17rv-3529dbk)</i> at a price of \$650, <i>Canon Powershot Digital Camera (sx40 hs)</i> at a price of \$380, etc
S_2	<i>Canon EOS DSLR Camera (T3i)</i> at a price of \$670, <i>Kodak Pocket Video Camera (Zi8)</i> at a price of \$240, <i>Brother Laser Printer (HL-2220)</i> at a price of \$90, etc

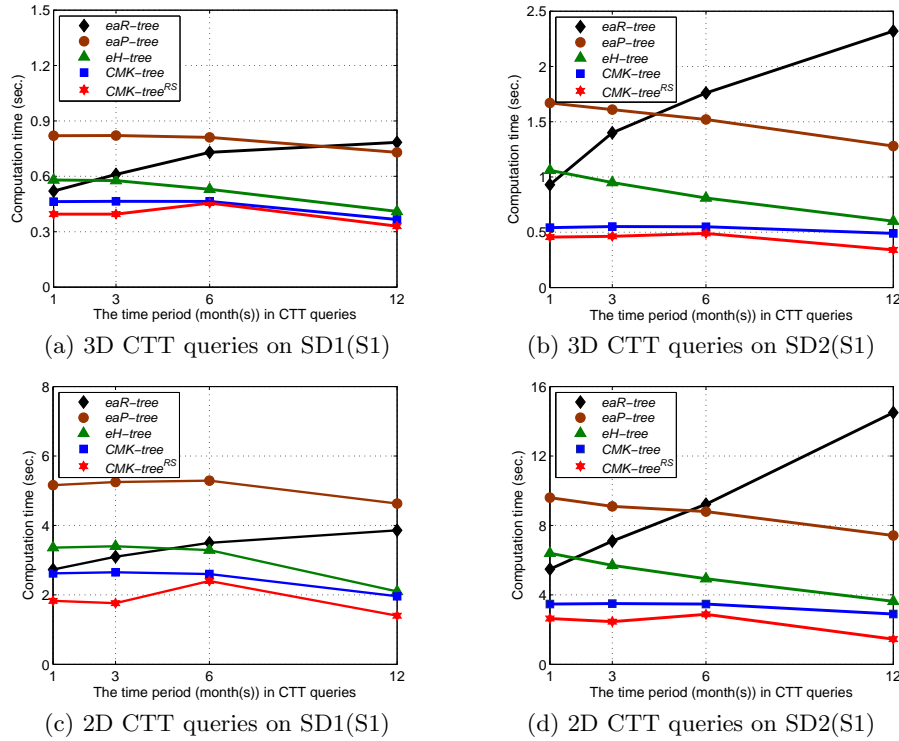


Figure 15: The query performance on two synthetic datasets SD1(S1) and SD2(S1) derived from seller S_1

queries, the *CMK-tree* reduces computation time by 66.7% of the *eaR-tree*, by 64.9% of the *eaP-tree*, and by 37.6% of the *eaH-tree*; for 180 2D CTT queries, the *CMK-tree* reduces computation time by 63.2% of the *eaR-tree*, by 61.8% of the *eaP-tree*, and by 35.4% of the *eaH-tree*.

From Figure 16 plotting the results executed on $SD_3(S_2)$ and $SD_4(S_2)$ for S_2 , we can draw the same conclusion as the results from datasets $SD_1(S_1)$ and $SD_2(S_1)$ for S_1 . On average, for 200 3D CTT queries based on Type I synthetic dataset $SD_3(S_2)$, the *CMK-tree* reduces computation time by 12.2% of the *eaR-tree*, by 41.1% of the *eaP-tree*, and by 20.0% of the *eaH-tree*; for 180 2D CTT queries, the *CMK-tree* reduces computation time by 15.6% of the *eaR-tree*, by 39.0% of the *eaP-tree*, and by 17.1% of the *eaH-tree*. On average, for 200 3D CTT queries based on Type II synthetic dataset $SD_4(S_2)$, the *CMK-tree* reduces computation time by 58.0% of the *eaR-tree*, by 54.4% of the *eaP-tree*, and by 28.1% of the *eaH-tree*; for 180 2D CTT queries, the *CMK-tree* reduces computation time by 59.8% of the *eaR-tree*, by 62.2% of the *eaP-tree*, and by 40.3% of the *eaH-tree*.

We also have tested the storage space consumption and I/O time for constructing these aggregation indexes over four synthetic datasets. As plotted in Fig. 17, the *CMK-tree* takes shorter time in construction than three existing approaches on four datasets (see Table 3 for detailed per-

centage). Overall, the proposed *CMK-tree* leads to 12%-84% time reduction in index construction. However, as plotted in Fig. 18, the *CMK-tree* consumes much storage space in some cases even if it aggregates repeated transactions (see Table 4 for detailed percentage). For example, on $SD_4(S_2)$ dataset, the *CMK-tree* increases 5%-35% in storage space consumption. This is because, in order to achieve nearly linear query performance, the *CMK-tree* continuously records the transactions whose generated intervals along the Transaction Time dimension intersect with the left border of a rectangle using multiple *aB⁺-trees*. Note that each rectangle is formed by a version of “domain 0” *K-D-B-tree* as shown in Fig. 11. In the next subsection, we will introduce the experimental results yield by our proposed *CMK-tree^{RS}*, which further reduces storage space consumption.

8.4 The Comparison of the CMK-tree and the CMK-tree^{RS}

Storage space reduction: Table 5 lists the percentage of storage space reduction of the *CMK-tree^{RS}* compared to the *CMK-tree*. Overall, the *CMK-tree^{RS}* reduces 23%-53% in storage space consumption on four datasets. On average, the reduction is about 38%.

As explained at the beginning of Section 7, if the ratings are aggregated at a coarse time granularity of months,

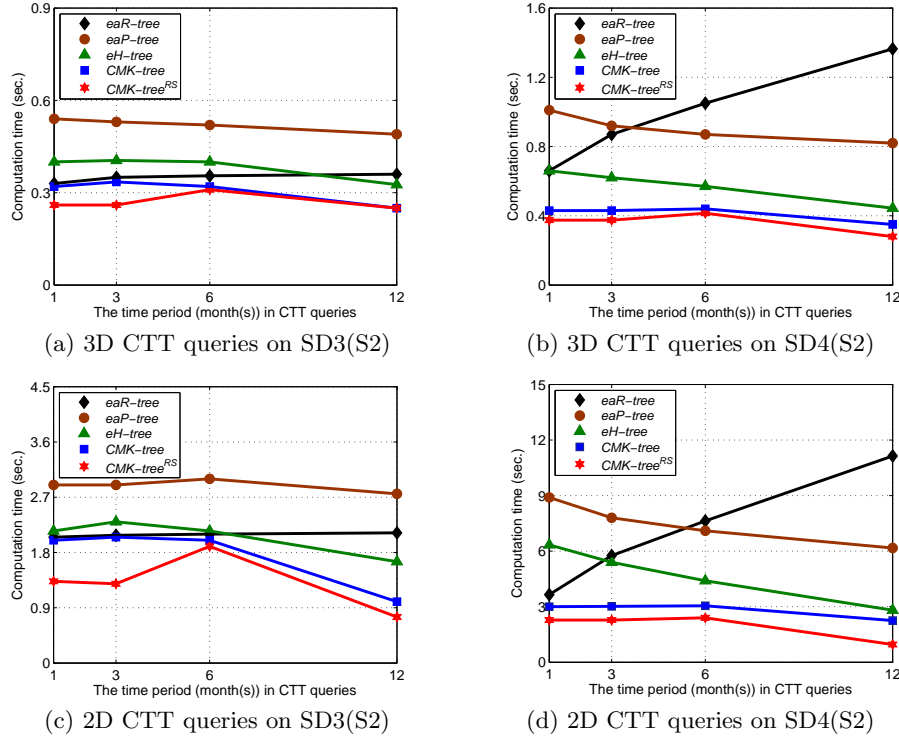


Figure 16: The query performance on two synthetic datasets SD3(S2) and SD4(S2) derived from seller S_2

Table 3: The comparison of constructing time between $CMK-tree$ and the existing index schemes over four synthetic datasets

	$SD1(S1)$	$SD2(S1)$	$SD3(S2)$	$SD4(S2)$
$CMK-tree$ vs. $eaR-tree$	18 : 100	21 : 100	34 : 100	16 : 100
$CMK-tree$ vs. $eaP-tree$	88 : 100	86 : 100	60 : 100	73 : 100
$CMK-tree$ vs. $eH-tree$	78 : 100	78 : 100	52 : 100	63 : 100

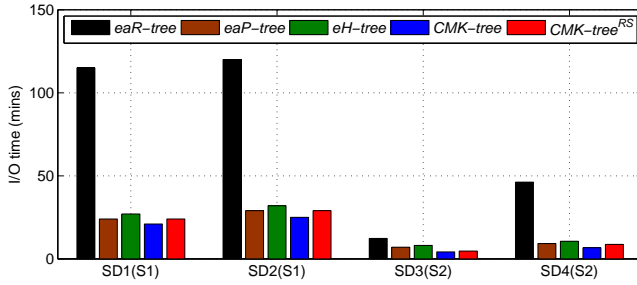


Figure 17: I/O time for different index schemes construction over four synthetic datasets

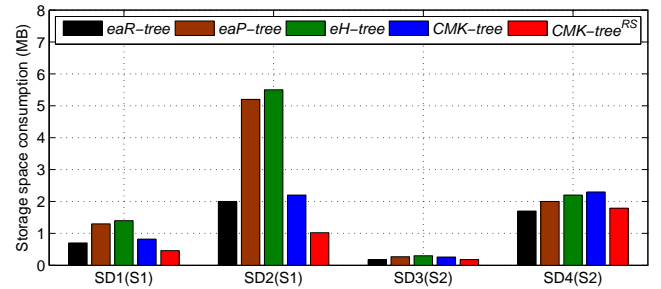


Figure 18: The storage space consumption for different index schemes over four synthetic datasets

the number of points in a two-dimensional space formed by transactions further decreases, since more repeated transactions exist in a month than on a day. Thus, the storage space consumption can be reduced.

Computation time improvement: The computation time of the two approaches are plotted in Figure 15 and Figure 16. In all cases, the $CMK-tree^{RS}$ is faster than the $CMK-tree$ in computing CTT values. On average, for the 200 3D CTT queries based on four datasets $SD1(S1)$, $SD2(S1)$, $SD3(S2)$ and $SD4(S2)$, the $CMK-tree^{RS}$ reduces computation time by 10.4%, 18.0%, 11.8% and 12.4% of the $CMK-tree$, respec-

tively; for the 180 2D CTT queries, the $CMK-tree^{RS}$ reduces computation time by 25.0%, 29.3%, 24.1% and 30.0% of the $CMK-tree$, respectively.

As explained in Section 7.2, when compared with the $CMK-tree$, the search in the $CMK-tree^{RS}$ for computing the left border VRA and the right border VRA is performed in two subtrees, i.e., $MK-tree^{day}$ and $MK-tree^{week}$, but they are much smaller in size than the original $MK-tree$ maintained in the $CMK-tree$. Thus, the search time can be reduced in computing two VRA queries.

Note that if the time range in a CTT query is “the latest

Table 4: The comparison of storage space consumption between *CMK-tree* and the existing index schemes over four synthetic datasets

	$SD1(S1)$	$SD2(S1)$	$SD3(S2)$	$SD4(S2)$
<i>CMK-tree</i> vs. <i>eaR-tree</i>	117 : 100	110 : 100	144 : 100	135 : 100
<i>CMK-tree</i> vs. <i>eaP-tree</i>	63 : 100	42 : 100	96 : 100	115 : 100
<i>CMK-tree</i> vs. <i>eH-tree</i>	59 : 100	40 : 100	87 : 100	105 : 100

Table 5: *CMK-tree* vs *CMK-tree*^{RS}

databases	percentage of storage space reduction	difference of CTT values
$SD1(S1)$	44%	minimal: 0% ; maximal: 0.15% ; average: 0.0018% ; error rate: 1.6%
$SD2(S1)$	53%	minimal: 0% ; maximal: 0.1% ; average: 0.0011% ; error rate: 1%
$SD3(S2)$	31%	minimal: 0% ; maximal: 2.8% ; average: 0.023% ; error rate: 4.2%
$SD4(S2)$	23%	minimal: 0% ; maximal: 0.34% ; average: 0.006% ; error rate: 3.2%

1 month” or “the latest 3 months”, only the *MK-tree*^{day} is searched for computing both the left border VRA and the right border VRA. Consequently, the *CMK-tree*^{RS} also delivers almost stable computation time for answering CTT queries at the above two time ranges. When the time range in CTT queries is “the latest 6 months”, the *MK-tree*^{day} is still searched for computing the right border VRA, but the *MK-tree*^{week} is searched for computing the left border VRA leading to a longer computation time¹⁰; therefore, we can observe that the computation time increases in this case for the *CMK-tree*^{RS}. However, if the time range in CTT queries is “the latest 12 months”, like the *eaP-tree*, the *eH-tree* and the *CMK-tree*, the computation time delivered by the *CMK-tree*^{RS} also drops to the minimum, since only a few nodes are visited for computing the left border VRA.

Difference in the accuracy of CTT values: In the meantime, as we have pointed out in Section 7, the *CMK-tree*^{RS} reduces storage space consumption at the expense of the accuracy of CTT values, which exists in the results of the CTT queries regarding “the latest 6 months” or “the latest 12 months”. Thus, we examined the differences of the results delivered by the *CMK-tree* and those by the *CMK-tree*^{RS} of the 95 CTT queries (i.e. 50 *3D CTT queries* and 45 *2D CTT queries*) regarding the above two time ranges, namely, totally 190 CTT queries are examined. Specifically, in Table 5, we listed the maximal, the minimal and the average differences as well as the error rate for the 190 CTT queries on four datasets. Overall, the *CMK-tree*^{RS} leads to 0.1%-2.8% in the maximal difference¹¹ of CTT values in [0, 1]. On average, the difference is 0.0011%-0.023%. In ad-

dition, the average error rate is 2.5%, i.e. 97.5% pairs of the results delivered by the *CMK-tree* and the *CMK-tree*^{RS} have the same values while 2.5% pairs have difference in the two values.

Therefore, we conclude that the *CMK-tree*^{RS} brings a very little loss to the accuracy of CTT computation with much gain in storage space reduction and computation time improvement.

9. CONCLUSION AND FUTURE WORK

In this paper, we have targeted the contextual transaction trust problem and proposed a novel and efficient model *ReputationPro* to compute and outline the reputation profile of a seller. It aims to identify the value imbalance problem and context imbalance problem in forthcoming transactions that can cause huge monetary losses of victims. In the meantime, it provides more comprehensive and detailed indications on the trust level of a seller. Our proposed index scheme *CMK-tree* takes into account both the static product category hierarchy and dynamic transaction amount and transaction time dimensions and achieves nearly linear query performance in answering a buyer’s CTT query. This is particularly significant to large-scale transaction data processing. In addition, our proposed *CMK-tree*^{RS} can further reduce the storage space allocated to each seller as well as the computation time for computing the CTT values. Furthermore, it loses very little accuracy for CTT computation.

For future work, we will focus on improving the performance of the *CMK-tree* in deletion. Given a transaction, its generated interval can intersect a number of rectangles until the time point “now”. Thus, when removing a transaction towards a *CMK-tree*, a lot of nodes that represent the corresponding rectangles have to be accessed leading to high complexity. In fact, in the *CMK-tree*, multiple *aB⁺-trees* are built to maintain the intersections between generated intervals and corresponding rectangles. Therefore, adding indexes to manage these *aB⁺-trees* separately would improve the performance of deletion operations.

10. REFERENCES

- [1] D. J. Abadi, S. R. Madden, and N. Hachem. Column-stores vs. row-stores: How different are they really. In *Proceedings of ACM SIGMOD*, 2008.

¹⁰The *MK-tree*^{day} maintains the aggregated ratings of the latest 3 months, and the *MK-tree*^{week} maintains the aggregated ratings of the remaining 9 months. Although 9 month transaction data and ratings are aggregated at a coarse time granularity of weeks in the *MK-tree*^{week}, it still has a larger size than *MK-tree*^{day}. Thus, the search in the *MK-tree*^{week} consumes more time than that in the *MK-tree*^{day}.

¹¹It can be expected that the maximal difference exists in computing the value of *3D CTT queries* with the parameter of product category at a low layer in the product category hierarchy, since a small amount of ratings involve in the computation. When performing “roll up” operations, more transaction data and ratings are involved in computation. As a result, the computation error rate can be reduced.

- [2] S. Ba and P. A. Pavlou. Evidence of the effect of trust building technology in electronic markets: Price premiums and buyer behavior. *MIS Quarterly*, 26(3):243–268, 2002.
- [3] R. Bayer and E. M. McCreight. Organization and maintenance of large ordered indices. *Acta Informatica*, 1:173–189, 1972.
- [4] B. Becker, S. Gschwind, T. Ohler, B. Seeger, and P. Widmayer. An asymptotically optimal multiversion b-tree. *Proceedings of The International Journal on Very Large Data Bases*, 5(4):264–275, 1996.
- [5] S. Chaudhuri and U. Dayal. An overview of data warehousing and olap technology. *SIGMOD Record*, 26(1):65–74, 1997.
- [6] E. Damiani, S. di Vimercati, S. Paraboschi, P. Samarati, and F. Violante. A reputation-based approach for choosing reliable resources in peer-to-peer networks. In *Proceedings of ACM conference on Computer and communications security*, pages 207–216, 2002.
- [7] E. Damiani, S. di Vimercati, P. Samarati, and M. Viviani. A wowa-based aggregation technique on trust values connected to metadata. *Electronic Notes in Theoretical Computer Science*, 157(3):131–142, 2006.
- [8] C. Dellarocas. Goodwill hunting: An economically efficient online feedback mechanism for environments with variable product quality. In *Workshop on Agent-Mediated Electronic Commerce*, pages 238–252, 2002.
- [9] J. Gray, S. Chaudhuri, A. Bosworth, A. Layman, D. Reichart, and M. Venkatrao. Data cube: A relational aggregation operator generalizing group-by, cross-tab, and subtotals. In *Proceedings of International Conference on Data Engineering*, pages 152–159, 1996.
- [10] N. Griffiths. Task delegation using experience-based multi-dimensional trust. In *Proceedings of ACM International Conference on Autonomous Agents and Multiagent Systems*, pages 489–496, 2005.
- [11] V. Harinarayan, A. Rajaraman, and J. D. Ullman. Implementing data cubes efficiently. In *Proceedings of ACM SIGMOD*, pages 205–216, 1996.
- [12] C. Jia, L. Xie, X. Gan, W. Liu, and Z. Han. A trust and reputation model considering overall peer consulting distribution. *IEEE Transactions on Systems, Man and Cybernetics, Part A: Systems and Humans*, 42(1):164–177, 2012.
- [13] A. Jøsang. Subjective evidential reasoning. In *Proceedings of the International Conference on Information Processing and Management of Uncertainty*, pages 1671–1678, 2002.
- [14] A. Jøsang, R. Ismail, and C. Boyd. A survey of trust and reputation systems for online service provision. *Decision Support Systems*, 43(2):618–644, 2007.
- [15] M. Jurgens and H.-J. Lenz. The ra*-tree: An improved r-tree with materialized data for supporting range queries on olap-data. In *Workshop on Database and Expert Systems Applications*, pages 186–191, Vienna, Austria, 1998.
- [16] S. Kamvar, M. Schlosser, and H. Garcia-Molina. The eigentrust algorithm for reputation management in p2p networks. In *Proceedings of International World Wide Web Conference*, pages 640–651, 2003.
- [17] S. T. Kang, Y. D. Chung, and M. H. Kim. An efficient method for temporal aggregation with range-condition attributes. *Information Sciences*, 168(1-4):243–265, 2004.
- [18] R. Kerr and R. Cohen. Modelling trust using transactional, numerical units. In *Proceedings of ACM International Conference on Privacy, Security and Trust*, 2006.
- [19] D. J. Kim, D. L. Ferrin, and H. R. Rao. A trust-based consumer decision-making model in electronic commerce: The role of trust, perceived risk, and their antecedents. *Decision Support Systems*, 44(2):342–353, 2008.
- [20] L. Li and Y. Wang. Context based trust normalization in service-oriented environments. In *Proceedings of IEEE International Conference on Autonomic and Trusted Computing*, pages 122–138, 2010.
- [21] M. Li, X. Sun, H. Wang, Y. Zhang, and J. Zhang. Privacy-aware access control with trust management in web service. *World Wide Web*, 14(4):407–430, 2011.
- [22] W.-Y. Lin and I.-C. Kuo. A genetic selection algorithm for olap data cubes. *Knowledge and Information Systems*, 6(1):83–102, 2004.
- [23] J. Liu and V. Issarny. Enhanced reputation mechanism for mobile ad hoc networks. In *Proceedings of International Conference on Trust Management*, pages 48–62, 2004.
- [24] X. Liu and A. Datta. Modeling context aware dynamic trust using hidden markov model. In *Proceedings of AAAI Conference on Artificial Intelligence*, pages 1938–1944, Toronto, Canada, 2012.
- [25] Z. Malik and A. Bouguettaya. Ratweb: Reputation assessment for trust establishment among web services. *The International Journal on Very Large Data Bases*, 18(4):885–911, 2009.
- [26] L. Mui. Computational models of trust and reputation: Agents, evolutionary games, and social networks. *PhD Thesis, University of MIT*, 2003.
- [27] D. Papadias, P. Kalnis, J. Zhang, and Y. Tao. Efficient olap operations in spatial data warehouses. In *Proceedings of International Symposium on Spatial and Temporal Databases*, pages 443–459, 2001.
- [28] D. Papadias, Y. F. Tao, P. Kalnis, and J. Zhang. Indexing spatio-temporal data warehouses. In *Proceedings of International Conference on Data Engineering*, pages 166–175, 2002.
- [29] M. Rehak, M. Pechoucek, and J. M. Bradshaw. Representing context for multiagent trust modeling. In *Proceedings of IEEE/WIC/ACM International Conference on Intelligent Agent Technology*, pages 737–746, 2006.
- [30] A. Rettinger, M. Nickles, and V. Tresp. Statistical relational learning of trust. *Machine learning*, 82(2):191–209, 2011.
- [31] B. Rietjens. Trust and reputation on ebay: Towards a legal framework for feedback intermediaries. *Information and Communications Technology Law.*, 15(1):55–78, 2006.
- [32] J. Robinson. The k-d-b-tree: A search structure for large multidimensional dynamic indexes. In

- Proceedings of ACM SIGMOD*, pages 10–18, 1981.
- [33] J. Sabater and C. Sierra. Regret: Reputation in gregarious societies. In *ACM AGENTS*, pages 194–195. ACM, 2001.
 - [34] S. Spitz and Y. Tüchtemann. A trust model considering the aspects of time. In *Proceedings of International Conference on Computer and Electrical Engineering*, pages 550–554, 2009.
 - [35] A. Swaminathan, R. G. Cattelan, Y. Wexler, C. V. Mathew, and D. Kirovski. Relating reputation and money in online markets. *ACM Transactions on the Web*, 4(4):1–31, 2010.
 - [36] Y. Tao and D. Papadias. Efficient aggregation over objects with extent. *ACM Transactions on Information Systems*, 23(1):61–102, 2005.
 - [37] Y. Tao, J. Zhang, D. Papadias, and N. Mamoulis. Range aggregate processing in spatial databases. *IEEE Transactions on Knowledge and Data Engineering*, 16(12):1555–1570, 2004.
 - [38] W. T. L. Teacy, J. Patel, N. R. Jennings, and M. Luck. Travos: Trust and reputation in the context of inaccurate information sources. *Autonomous Agents and Multi-Agent Systems*, 12(2):183–198, 2006.
 - [39] M. Uddin, M. Zulkernine, and S. Ahamed. Cat: A context-aware trust model for open and dynamic systems. In *Proceedings of ACM Symposium on Applied Computing*, pages 2024–2029, 2008.
 - [40] L.-H. Vu, M. Hauswirth, and K. Aberer. Qos-based service selection and ranking with trust and reputation management. In *Proceedings of IEEE International Conference on Cooperative information system*, pages 466–483, 2005.
 - [41] X. F. Wang, L. Liu, and J. Su. Rlm: A general model for trust representation and aggregation. *IEEE Transaction on Service Computing*, 5(1):131–143, 2012.
 - [42] Y. Wang and L. Li. Two-dimensional trust rating aggregations in service-oriented applications. *IEEE Transactions on Service Computing*, 4(4):257–271, 2011.
 - [43] Y. Wang and E.-P. Lim. The evaluation of situational transaction trust in e-service environments. In *Proceedings of IEEE International Conference of Engineering and Business Education*, pages 265–272, 2008.
 - [44] Y. Wang and K.-J. Lin. Reputation-oriented trustworthy computing in e-commerce environments. *IEEE Internet Computing*, 12(4):55–59, 2008.
 - [45] Y. Wang, K.-J. Lin, D. S. Wong, and V. Varadharajan. Trust management towards service-oriented applications. *Service Oriented Computing and Applications Journal*, 3(2):129–146, 2009.
 - [46] Y. Wang and M. P. Singh. Formal trust model for multiagent systems. In *Proceedings International Joint Conference on Artificial Intelligence*, pages 1551–1556, 2007.
 - [47] Y. Wang and V. Varadharajan. Trust²: Developing trust in peer-to-peer environments. In *Proceedings of International Conference on Services Computing*, pages 24–31, 2005.
 - [48] Y. Wang and V. Varadharajan. Two-phase peer evaluation in p2p e-commerce environments. In *Proceedings of International Conference on e-Technology, e-Commerce and e-Service*, pages 654–657, 2005.
 - [49] L. Xiong and L. Liu. A reputation-based trust model for peer-to-peer ecommerce communities. In *IEEE International Conference on E-Commerce*, pages 275–284, 2003.
 - [50] L. Xiong and L. Liu. Peertrust: Supporting reputation-based trust in peer-to-peer communities. *IEEE Transactions on Knowledge and Data Engineering*, 16(7):843–857, 2004.
 - [51] J. Yang and J. Widom. Incremental computation and maintenance of temporal aggregates. *Proceedings of International Conference on Very Large Data Bases*, 12(3):262–283, 2003.
 - [52] G. Zacharia and P. Maes. Trust management through reputation mechanisms. *Applied Artificial Intelligence*, 14(9):881–907, 2000.
 - [53] D. Zhang, D. Gunopulos, V. J. Tsotras, and B. Seeger. Temporal and spatio-temporal aggregations over data streams using multiple time granularities. *Information System*, 28(1-2):61–84, 2003.
 - [54] D. Zhang, A. Markowetz, V. J. Tsotras, D. Gunopulos, and B. Seeger. Efficient computation of temporal aggregates with range predicates. In *Proceedings of ACM International Symposium on Principles of Database Systems*, pages 237–245, 2001.
 - [55] D. Zhang, A. Markowetz, V. J. Tsotras, D. Gunopulos, and B. Seeger. Efficient aggregation over objects with extent. In *Proceedings of ACM International Symposium on Principles of Database Systems*, pages 121–132, 2002.
 - [56] D. Zhang, A. Markowetz, V. J. Tsotras, D. Gunopulos, and B. Seeger. On computing temporal aggregates with range predicates. *ACM Transactions on Database Systems*, 33(2):1–38, 2008.
 - [57] H. Zhang and Y. Wang. A novel model for contextual transaction trust computation with fixed storage space in e-commerce and e-service environments. In *Proceedings of IEEE International Conference on Services Computing*, pages 667–674, 2013.
 - [58] H. Zhang, Y. Wang, and X. Zhang. Transaction similarity-based contextual trust evaluation in e-commerce and e-service environments. In *Proceedings of IEEE International Conference on Web Services*, pages 500–507, 2011.
 - [59] H. Zhang, Y. Wang, and X. Zhang. Efficient contextual transaction trust computation in e-commerce environments. In *Proceedings of IEEE International Conference on Trust, Security and Privacy in Computing and Communications*, pages 318–325, 2012.
 - [60] H. Zhang, Y. Wang, and X. Zhang. A trust vector approach to transaction context-aware trust evaluation in e-commerce and e-service environments. In *Proceedings of IEEE International Conference on Service Oriented Computing and Applications*, pages 1–8, 2012.
 - [61] H. Zhang, Y. Wang, and X. Zhang. The approaches to contextual transaction trust computation in e-commerce environments. *Security and*

Communication Networks Journal, 2013. in press.

